Valence bond solids for SU(n) spin chains: Exact models, spinon confinement, and the Haldane gap

Martin Greiter and Stephan Rachel

Institut für Theorie der Kondensierten Materie, Universität Karlsruhe, Postfach 6980, 76128 Karlsruhe, Germany
(Received 19 January 2007; revised manuscript received 10 April 2007; published 31 May 2007)

To begin with, we introduce several exact models for SU(3) spin chains: First is a translationally invariant parent Hamiltonian involving four-site interactions for the trimer chain, with a threefold degenerate ground state. We provide numerical evidence that the elementary excitations of this model transform under representation $\bar{\mathbf{3}}$ of SU(3) if the original spins of the model transform under representation **3**. Second is a family of parent Hamiltonians for valence bond solids of SU(3) chains with spin representations **6**, **10**, and **8** on each lattice site. We argue that of these three models, only the latter two exhibit spinon confinement and, hence, a Haldane gap in the excitation spectrum. We generalize some of our models to SU(n). Finally, we use the emerging rules for the construction of valence bond solid states to argue that models of antiferromagnetic chains of SU(n) spins, in general, possess a Haldane gap if the spins transform under a representation corresponding to a Young tableau consisting of a number of boxes λ which is divisible by n. If λ and n have no common divisor, the spin chain will support deconfined spinons and not exhibit a Haldane gap. If λ and n have a common divisor different from n, it will depend on the specifics of the model including the range of the interaction.

I. INTRODUCTION

Quantum spin chains have been a most rewarding subject of study almost since the early days of quantum mechanics, beginning with the invention of the Bethe ansatz in 1931 (Ref. [1]) as a method of solving the $S=\frac{1}{2}$ Heisenberg chain with nearest-neighbor interactions. The method led to the discovery of the Yang-Baxter equation in 1967 (Refs. [2] and [3]) and provides the foundation for the field of integrable models.[4] Faddeev and Takhtajan[5] discovered in 1981 that the elementary excitations (now called spinons) of the spin-1/2 Heisenberg chain carry spin 1/2 while the Hilbert space is spanned by spin flips, which carry spin 1. The fractional quantization of spin in spin chains is conceptually similar to the fractional quantization of charge in quantized Hall liquids.[6,7] In 1982, Haldane[8,9] identified the O(3) nonlinear sigma model as the effective low-energy field theory of SU(2) spin chains and argued that chains with integer spin possess a gap in the excitation spectrum, while a topological term renders half-integer spin chains gapless.[10,11]

The general methods—the Bethe ansatz method and the use of effective field theories including bosonization[12,13]—are complemented by a number of exactly solvable models; most prominently among them are the Majumdar-Ghosh (MG) Hamiltonian for the $S=\frac{1}{2}$ dimer chain,[14] the AKLT model as a paradigm of the gapped $S=1$ chain,[15,16] and the Haldane-Shastry model (HSM).[17–20] The HSM is by far the most sophisticated among these three, as it is not only solvable for the ground state but fully integrable due to its Yangian symmetry.[20] The wave functions for the ground state and single-spinon excitations are of a simple Jastrow form, elevating the conceptual similarity to quantized Hall states to a formal equivalence. Another unique feature of the HSM is that the spinons are free in the sense that they only interact through their half-Fermi statistics,[21–25] which renders model an ideal starting point for any perturbative description

of spin systems in terms of interacting spinons.[26] The HSM has been generalized from SU(2) to SU(n).[27–32]

For the MG and the AKLT model, only the ground states are known exactly. Nonetheless, these models have amply contributed to our understanding of many aspects of spin chains, each of them through the specific concepts captured in its ground state.[33–51] The models are specific to SU(2) spin chains. We will review both models below.

In the past, the motivation to study SU(n) spin systems with $n>2$ has been mainly formal. The Bethe ansatz method has been generalized to multiple-component systems by Sutherland,[52] yielding the so-called nested Bethe ansatz. In particular, this has led to a deeper understanding of quantum integrability and the applicability of the Bethe ansatz.[53] Furthermore, the nested Bethe ansatz was used to study the spectrum of the SU(n) HSM.[22,27] It has also been applied to SU(2) spin chains with orbital degeneracy at the SU(4) symmetric point.[54,55] Most recently, Damerau and Klümper obtained highly accurate numerical results for the thermodynamic properties of the SU(4) spin-orbital model.[56] SU(n) Heisenberg models have been studied recently by Kawashima and Tanabe[57] with quantum Monte Carlo and by Paramekanti and Marston[58] using variational wave functions.

The effective field theory description of SU(2) spin chains by Haldane yielding the distinction between gapless half-integer spin chains with deconfined spinons and gapped integer spin chains with confined spinons cannot be directly generalized to SU(n), as there is no direct equivalent of the CP^1 representation used in Haldane's analysis. The critical behavior of SU(n) spin chains, however, has been analyzed by Affleck in the framework of effective field theories.[59,60]

An experimental realization of an SU(3) spin system and, in particular, an antiferromagnetic SU(3) spin chain, however, might be possible in an optical lattice of ultracold atoms in the not-too-distant future. The "spin" in these systems would, of course, not relate to the rotation group of our

physical space but rather relate to SU(3) rotations in an internal space spanned by three degenerate "colors" the atom may assume, subject to the requirement that the number of atoms of each color is conserved. A possible way to realize such a system experimentally is described in Appendix A. Moreover, it has been suggested recently that an SU(3) trimer state might be realized approximately in a spin tetrahedron chain.[61,62]

Motivated by both this prospect as well as the mathematical challenges inherent to the problem, we propose several exact models for SU(3) spin chains in this paper. The models are similar in spirit to the MG or the AKLT model for SU(2) and consist of parent Hamiltonians and their exact ground states. There is no reason to expect any of these models to be integrable, and none of the excited states are known exactly. We generalize several of our models to SU(n) and use the emerging rules to investigate and motivate which SU(n) spin chains exhibit spinon confinement and a Haldane gap.

The paper is organized as follows. Following a brief review of the MG model in Sec. II, we introduce the trimer model for SU(3) spin chains in Sec. III. This model consists of a translationally invariant Hamiltonian involving four-site interactions, with a threefold degenerate ground state, in which triples of neighboring sites form SU(3) singlets (or trimers). In Sec. IV, we review the representations of SU(3), which we use to verify the trimer model in Sec. V. In this section, we further provide numerical evidence that the elementary excitations of this model transform under representation $\overline{\mathbf{3}}$ of SU(3) if the original spins of the model transform under representation $\mathbf{3}$. We proceed by introducing Schwinger bosons in Sec. VI and a review of the AKLT model in Sec. VII. In Sec. VIII, we formulate a family of parent Hamiltonians for valence bond solids of SU(3) chains with spin representations $\mathbf{6}$, $\mathbf{10}$, and $\mathbf{8}$ on each lattice site and prove their validity. We argue that only the representation $\mathbf{10}$ and the representation $\mathbf{8}$ model, which are in a wider sense generalizations of the AKLT model to SU(3), exhibit spinon confinement and, hence, a Haldane-type gap in the excitation spectrum. In Sec. IX, we generalize three of our models from SU(3) to SU(n). In Sec. X, we use the rules emerging from the numerous valence bond solid (VBS) models we studied to investigate which models of SU(n) spin chains, in general, exhibit spinon confinement and a Haldane gap. In this context, we first review a rigorous theorem due to Affleck and Lieb[63] in Sec. X A. In Sec. X B, we argue that the spinons in SU(n) spin chains with spins transforming under representations with Young tableaux consisting of a number of boxes λ which is divisible by n are always confined. In Sec. X C, we construct several specific examples to argue that if λ and n have a common divisor different from n, the model will be confining only if the interactions are sufficiently long ranged. Specifically, the models we study suggest that if q is the largest common divisor of λ and n, the model will exhibit spinon confinement only if the interactions extend at least to the (n/q)th neighbor on the chain. If λ and n have no common divisor, the spinons will be free and the chain will not exhibit a Haldane gap. We briefly summarize the different categories of models in Sec. X D and present a counterexample to the general rules in Sec. X E. We conclude with a brief summary of the results obtained in this paper in Sec. XI.

A brief and concise account of the SU(3) VBS models we elaborate here has been given previously.[64]

II. MAJUMDAR-GHOSH MODEL

Majumdar and Ghosh[14] noticed in 1969 that on a linear spin $S=\frac{1}{2}$ chain with an even number of sites, the two valence bond solid or dimer states

$$|\psi_{\mathrm{MG}}^{\overset{\mathrm{even}}{(\mathrm{odd})}}\rangle = \prod_{\substack{i\ \mathrm{even} \\ (i\ \mathrm{odd})}} \left(c_{i\uparrow}^{\dagger} c_{i+1\downarrow}^{\dagger} - c_{i\downarrow}^{\dagger} c_{i+1\uparrow}^{\dagger} \right) |0\rangle =$$

$$= \begin{cases} |\ \circ\!\!-\!\!\circ\ \ \circ\!\!-\!\!\circ\ \ \circ\!\!-\!\!\circ\ \ \circ\ \rangle & \text{``even''} \\ |\ \circ\ \ \circ\!\!-\!\!\circ\ \ \circ\!\!-\!\!\circ\ \ \circ\!\!-\!\!\circ\ \rangle & \text{``odd''} \end{cases} \tag{1}$$

where the product runs over all even sites i for one state and over all odd sites for the other, are exact zero-energy ground states[65] of the parent Hamiltonian

$$H_{\mathrm{MG}} = \sum_i \left(S_i S_{i+1} + \frac{1}{2} S_i S_{i+2} + \frac{3}{8} \right), \tag{2}$$

where

$$S_i = \frac{1}{2} \sum_{\tau,\tau'=\uparrow,\downarrow} c_{i\tau}^{\dagger} \boldsymbol{\sigma}_{\tau\tau'} c_{i\tau'}, \tag{3}$$

and $\boldsymbol{\sigma}=(\sigma_x,\sigma_y,\sigma_z)$ is the vector consisting of the three Pauli matrices.

The proof is exceedingly simple. We rewrite

$$H_{\mathrm{MG}} = \frac{1}{4}\sum_i H_i, \quad H_i = (S_i + S_{i+1} + S_{i+2})^2 - \frac{3}{4}. \tag{4}$$

Clearly, any state in which the total spin of three neighboring spins is $\frac{1}{2}$ will be annihilated by H_i. (The total spin can only be $\frac{1}{2}$ or $\frac{3}{2}$, as $\frac{1}{2}\otimes\frac{1}{2}\otimes\frac{1}{2}=\frac{1}{2}\oplus\frac{1}{2}\oplus\frac{3}{2}$.) In the dimer states above, this is always the case as two of the three neighboring spins are in a singlet configuration, and $\mathbf{0}\otimes\frac{1}{2}=\frac{1}{2}$. Graphically, we may express this as

$$H_i\,|\,\circ\!\!-\!\!\circ\ \ \circ\ \rangle = H_i\,|\,\circ\ \ \circ\!\!-\!\!\circ\ \rangle = 0. \tag{5}$$

As H_i is positive definite, the two zero-energy eigenstates of H_{MG} are also ground states.

Is the Majumdar-Ghosh or dimer state in the universality class generic to one-dimensional spin-$\frac{1}{2}$ liquids, and hence a useful paradigm to understand, say, the nearest-neighbor Heisenberg chain? The answer is clearly no, as the dimer states [Eq. (1)] violate translational symmetry modulo translations by two lattice spacings, while the generic liquid is invariant.

Nonetheless, the dimer chain shares some important properties of this generic liquid. First, the spinon excitations—here, domain walls between even and odd ground states—are deconfined. (To construct approximate eigenstates of H_{MG},

we take momentum superpositions of localized domain walls.) Second, there are (modulo the overall twofold degeneracy) only $M+1$ orbitals available for an individual spinon if $2M$ spins are condensed into dimers or valence bond singlets. This is to say that if there are only a few spinons in a long chain, the number of orbitals available to them is roughly half the number of sites. This can easily be seen graphically:

If we start with an even ground state on the left, the spinon to its right must occupy an even lattice site and vice versa. The resulting state counting is precisely what one finds in the Haldane-Shastry model, where it is directly linked to the half-Fermi statistics of the spinons.[21]

The dimer chain is further meaningful as a piece of a general paradigm. The two degenerate dimer states [Eq. (1)] can be combined into an $S=1$ chain, the AKLT chain, which serves as a generic paradigm for $S=1$ chains which exhibit the Haldane gap[8,9,34] and provides the intellectual background for several of the exact models we further introduce below. Before doing so, however, we will now introduce the trimer model, which constitutes an SU(3) analog of the MG model.

III. TRIMER MODEL

A. Hamiltonian and its ground states

Consider a chain with N lattice sites, where N has to be divisible by 3, and periodic boundary conditions (PBCs). On each lattice site, we place an SU(3) spin which transforms under the fundamental representation **3**, i.e., the spin can take the values (or colors) blue (b), red (r), or green (g). The trimer states are obtained by requiring the spins on each three neighboring sites to form an SU(3) singlet, which we call a trimer and sketch it by ∘–∘–∘. The three linearly independent trimer states on the chain are given by

$$
\left| \psi_{\text{trimer}}^{(\mu)} \right\rangle =
\begin{cases}
\left| \text{ ∘–∘–∘ ∘–∘–∘ } \right\rangle \equiv \left| \psi_{\text{trimer}}^{(1)} \right\rangle \\[4pt]
\left| \text{ ∘ ∘–∘–∘ ∘–∘ } \right\rangle \equiv \left| \psi_{\text{trimer}}^{(2)} \right\rangle \\[4pt]
\left| \text{ ∘–∘ ∘–∘–∘ ∘ } \right\rangle \equiv \left| \psi_{\text{trimer}}^{(3)} \right\rangle .
\end{cases}
$$
(6)

Introducing operators $c_{i\sigma}^{\dagger}$ which create a fermion of color σ ($\sigma = \text{b,r,g}$) at lattice site i, the trimer states can be written as

$$
\left| \psi_{\text{trimer}}^{(\mu)} \right\rangle \\
= \prod_{\substack{i \\ [(i-\mu)/3 \text{ integer}]}} \left(\sum_{(\alpha,\beta,\gamma) = \pi(\text{b,r,g})} \text{sgn}(\pi) c_{i\alpha}^{\dagger} c_{i+1\beta}^{\dagger} c_{i+2\gamma}^{\dagger} \right) |0\rangle,
$$
(7)

where $\mu = 1,2,3$ labels the three degenerate ground states, and i runs over the lattice sites subject to the constraint that $\frac{i-\mu}{3}$ is integer. The sum extends over all six permutations π of the three colors b, r, and g, i.e.,

$$
\sum_{(\alpha,\beta,\gamma)=\pi(\text{b,r,g})} \text{sgn}(\pi) c_{i\alpha}^{\dagger} c_{i+1\beta}^{\dagger} c_{i+2\gamma}^{\dagger} = c_{ib}^{\dagger} c_{i+1r}^{\dagger} c_{i+2g}^{\dagger} + c_{ir}^{\dagger} c_{i+1g}^{\dagger} c_{i+2b}^{\dagger} + c_{ig}^{\dagger} c_{i+1b}^{\dagger} c_{i+2r}^{\dagger} - c_{ib}^{\dagger} c_{i+1g}^{\dagger} c_{i+2r}^{\dagger} - c_{ig}^{\dagger} c_{i+1r}^{\dagger} c_{i+2b}^{\dagger} - c_{ir}^{\dagger} c_{i+1b}^{\dagger} c_{i+2g}^{\dagger}. \quad (8)
$$

The SU(3) generators at each lattice site i are in analogy to Eq. (3) defined as

$$
J_i^a = \frac{1}{2} \sum_{\sigma,\sigma'=\text{b,r,g}} c_{i\sigma}^{\dagger} \lambda_{\sigma\sigma'}^a c_{i\sigma'}, \quad a = 1,\ldots,8,
$$
(9)

where the λ^a are the Gell-Mann matrices (see Appendix B). The operators [Eq. (9)] satisfy the commutation relations

$$
[J_i^a, J_j^b] = \delta_{ij} f^{abc} J_i^c, \quad a,b,c = 1,\ldots,8,
$$
(10)

(we use the Einstein summation convention) with f^{abc} the structure constants of SU(3) (see Appendix B). We further introduce the total SU(3) spin of ν neighboring sites $i,\ldots,i+\nu-1$,

$$
\boldsymbol{J}_i^{(\nu)} = \sum_{j=i}^{i+\nu-1} \boldsymbol{J}_j,
$$
(11)

where $\boldsymbol{J}_i$ is the eight-dimensional vector formed by its components [Eq. (9)]. The parent Hamiltonian for the trimer states [Eq. (7)] is given by

$$
H_{\text{trimer}} = \sum_{i=1}^{N} \left(\left(\boldsymbol{J}_i^{(4)} \right)^4 - \frac{14}{3} \left(\boldsymbol{J}_i^{(4)} \right)^2 + \frac{40}{9} \right).
$$
(12)

The $\boldsymbol{J}_i \boldsymbol{J}_j$ terms appear complicated in terms of the Gell-Mann matrices but are rather simply when written out using the operator P_{ij}, which permutes the SU(n) spins (here, $n=3$) on sites i and j:

$$
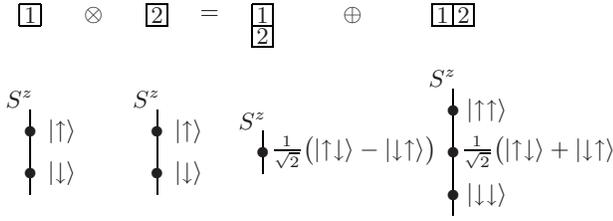\boldsymbol{J}_i \boldsymbol{J}_j = \frac{1}{2}\left(P_{ij} - \frac{1}{n} \right).
$$
(13)

FIG. 1. Tensor product of two $S=\frac{1}{2}$ spins with Young tableaux and weight diagrams of the occurring SU(2) representations. S^z is the diagonal generator.

To verify the trimer Hamiltonian [Eq. (12)], as well as for the valence bond solid (VBS) models we propose below, we will need a few higher-dimensional representations of SU(3). We review these in the following section.

IV. REPRESENTATIONS OF SU(3)

A. Young tableaux and representations of SU(2)

Let us begin with a review of Young tableaux and the representations of SU(2). The group SU(2) has three generators S^a, $a=1,2,3$, which obey the algebra

$$[S^a, S^b] = i\epsilon^{abc}S^c, \qquad (14)$$

where repeated indices are summed over and ϵ^{abc} is the totally antisymmetric tensor. The representations of SU(2) are classified by the spin S, which takes integer or half-integer values. The fundamental representation of SU(2) has spin $S = \frac{1}{2}$; it contains the two states $|\uparrow\rangle$ and $|\downarrow\rangle$. Higher-dimensional representations can be constructed as tensor products of fundamental representations, which is conveniently accomplished using Young tableaux (see, e.g., Ref. 66). These tableaux are constructed as follows (see Figs. 1 and 2 for examples). For each of the N spins, draw a box numbered consecutively from left to right. The representations of SU(2) are obtained by putting the boxes together such that the numbers assigned to them increase in each row from left to right and in each column from top to bottom. Each tableau indicates symmetrization over all boxes in the same row and antisymmetrization over all boxes in the same column. This implies that we cannot have more than two boxes on top of each other. If κ_i denotes the number of boxes in the ith row, the spin is given by $S=\frac{1}{2}(\kappa_1 - \kappa_2)$.

To be more explicit, let us consider the tensor product $\frac{1}{2} \otimes \frac{1}{2} \otimes \frac{1}{2}$ depicted in Fig. 2 in detail. We start with the state $|\frac{3}{2},\frac{3}{2}\rangle = |\uparrow\uparrow\uparrow\rangle$ and hence find

FIG. 2. Tensor product of three $S=\frac{1}{2}$ spins with Young tableaux. For SU(n) with $n>2$, the tableau with three boxes on top of each other exists as well.
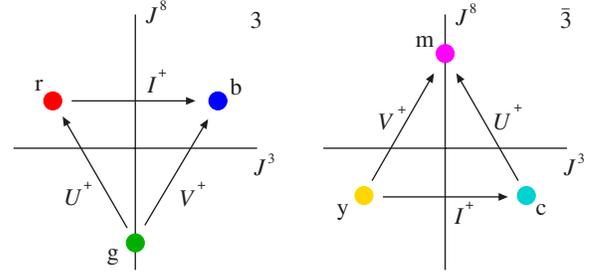

FIG. 3. (Color online) (a) Weight diagram of the fundamental SU(3) representation $\mathbf{3}=(1,0)$. (b) Weight diagram of the complex conjugate representation $\bar{\mathbf{3}}=(0,1)$. J^3 and J^8 denote the diagonal generators, I^+, U^+, and V^+ the raising operators.

$$\left|\frac{3}{2},\frac{1}{2}\right\rangle = \frac{1}{\sqrt{3}}S^-\left|\frac{3}{2},\frac{3}{2}\right\rangle = \frac{1}{\sqrt{3}}(|\uparrow\uparrow\downarrow\rangle + |\uparrow\downarrow\uparrow\rangle + |\downarrow\uparrow\uparrow\rangle). \quad (15)$$

The two states with $S=S^z=\frac{1}{2}$ must be orthogonal to Eq. (15). A convenient choice of basis is

$$\left|\frac{1}{2},\frac{1}{2},+\right\rangle = \frac{1}{\sqrt{3}}(|\uparrow\uparrow\downarrow\rangle + \omega|\uparrow\downarrow\uparrow\rangle + \omega^2|\downarrow\uparrow\uparrow\rangle),$$

$$\left|\frac{1}{2},\frac{1}{2},-\right\rangle = \frac{1}{\sqrt{3}}(|\uparrow\uparrow\downarrow\rangle + \omega^2|\uparrow\downarrow\uparrow\rangle + \omega|\downarrow\uparrow\uparrow\rangle), \quad (16)$$

where $\omega=\exp(i\frac{2\pi}{3})$. The tableaux tell us primarily that two such basis states exist, and not what a convenient choice of orthonormal basis states may be.

The irreducible representations of SU(2) can be classified through the eigenvalues of the Casimir operator given by the square of the total spin $\mathbf{S}^2$. The special feature of $\mathbf{S}^2$ is that it commutes with all generators S^a and is, hence, by Schur's lemma[67] proportional to the identity for any finite-dimensional irreducible representation. The eigenvalues are given by

$$\mathbf{S}^2 = \mathcal{C}^2_{\text{SU}(2)} = S(S+1).$$

B. Representation theory of SU(3)

The group SU(3) has eight generators J^a, $a=1,\ldots,8$, which obey the algebra

$$[J^a, J^b] = f^{abc}J^c, \qquad (17)$$

where the structure constants f^{abc} are given in Appendix B. For SU(3), we have two diagonal generators, usually chosen to be J^3 and J^8, and six generators which define the ladder operators $I^\pm = J^1 \pm iJ^2$, $U^\pm = J^6 \pm iJ^7$, and $V^\pm = J^4 \pm iJ^5$, respectively. An explicit realization of Eq. (17) is, for example, given by the J^a's as expressed in terms of the Gell-Mann matrices in Eq. (9). This realization defines the fundamental representation $\mathbf{3}$ of SU(3) illustrated in Fig. 3(a). It is three dimensional, and we have chosen to label the basis states by the colors blue (b), red (r), and green (g). The weight diagram depicted in Fig. 3(a) instructs us about the eigenvalues of the diagonal generators as well as the actions of the ladder operators on the basis states.
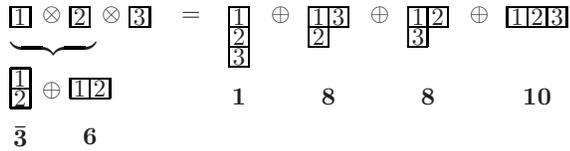
FIG. 4. Tensor product **3**⊗**3**⊗**3** with Young tableaux.

All other representations of SU(3) can be constructed by taking tensor products of representations **3**, which is again most conveniently accomplished using Young tableaux (see Fig. 4 for an example). The antisymmetrization over all boxes in the same column implies that we cannot have more than three boxes on top of each other. Each tableau stands for an irreducible representation of SU(3), which can be uniquely labeled by their highest weight or Dynkin coordinates (μ_1,μ_2) Refs. 67 and 68 (see Fig. 5). For example, the fundamental representation **3** has Dynkin coordinates (1,0). Note that all columns containing three boxes are superfluous, as the antisymmetrization of three colors yields only one state. In particular, the SU(3) singlet has Dynkin coordinates (0,0). In general, the dimension of a representation (μ_1,μ) is given by $\frac{1}{2}(\mu_1+1)(\mu_2+1)(\mu_1+\mu_2+2)$. The labeling using numbers in boldface refers to the dimensions of the representations alone. Although this labeling is not unique, it will mostly be sufficient for our purposes. A representation **m** and its conjugated counterpart **m̄** are related to each other by interchange of their Dynkin coordinates.

C. Examples of representations of SU(3)

We now consider some specific representations of SU(3) in detail. As starting point, we use the fundamental representation **3** spanned by the states $|b\rangle$, $|r\rangle$, and $|g\rangle$. The second three-dimensional representation **3̄** is obtained by antisymmetrically coupling two representations **3**. The Dynkin coordinates of the representations **3̄** are (0,1), i.e., the representations **3** and **3̄**, are complex conjugate of each other. An explicit basis of the representations **3̄** is given by the colors yellow (y), cyan (c), and magenta (m) as follows:

$$|y\rangle = \frac{1}{\sqrt{2}}(|rg\rangle - |gr\rangle),$$

$$|c\rangle = \frac{1}{\sqrt{2}}(|gb\rangle - |bg\rangle),$$
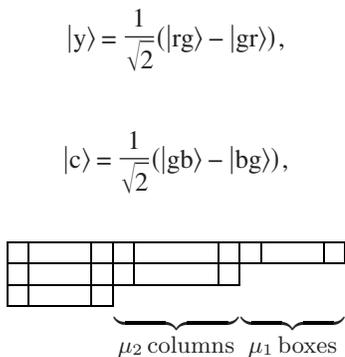

$$\mu_2 \text{ columns} \quad \mu_1 \text{ boxes}$$

FIG. 5. Dynkin coordinates (μ_1,μ_2) for a given Young tableau. The columns containing three boxes represent additional SU(3) singlet factors, which yield equivalent representations and hence leave the Dynkin coordinates (μ_1,μ_2) unchanged.
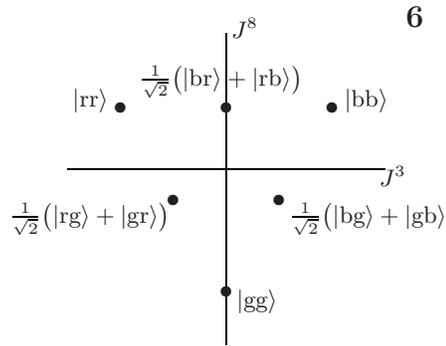

FIG. 6. Weight diagram of the representation **6**=(2,0). The weight diagram of the conjugate representation **6̄**=(0,2) is obtained by reflection at the origin (Ref. 67).

$$|m\rangle = \frac{1}{\sqrt{2}}(|br\rangle - |rb\rangle). \tag{18}$$

The weight diagram is shown in Fig. 3(b). The generators are given by Eq. (9) with λ^a replaced by $-(\lambda^a)^*$, where asterisk (∗) denotes complex conjugation of the matrix elements.[68] In particular, we find $I^+|y\rangle = -|c\rangle$, $U^+|c\rangle = -|m\rangle$, and $V^+|y\rangle = -|m\rangle$.

The six-dimensional representation **6** has Dynkin coordinates (2,0) and can, hence, be constructed by symmetrically coupling two representations **3**. The basis states of the representations **6** are shown in Fig. 6. The conjugate representation **6̄** can be constructed by symmetrically coupling two representations **3̄**.

Let us now consider the tensor product **3**⊗**3̄**=**1**⊕**8**. The weight diagram of the so-called adjoint representation **8** =(1,1) is shown in Fig. 7. The states can be constructed starting from the highest weight state $|bm\rangle$, yielding $I^-|bm\rangle = |rm\rangle$, $U^-|bm\rangle = -|bc\rangle$, $V^-|bm\rangle = |gm\rangle - |by\rangle$, and so on. This procedure yields two linearly independent states with $J^3 = J^8 = 0$. The representation **8** can also be obtained by cou-

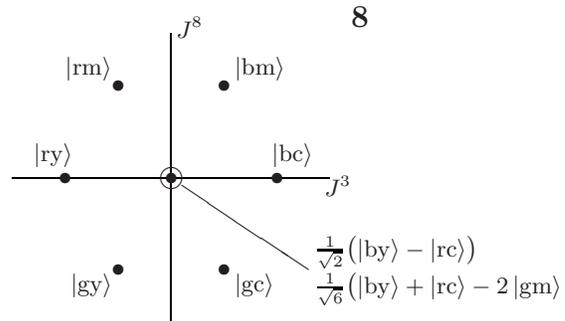FIG. 7. Weight diagram of the adjoint representation **8**=(1,1). The state with $J^3 = J^8 = 0$ is doubly degenerate (Ref. 67). Note that two representations **8** can be constructed by combining three fundamental representations **3** (colors), just as two representations $\frac{1}{2}$ can be constructed by combining three SU(2) spins [cf. Eq. (16)]. The states in the diagram span a basis for one of these representations.
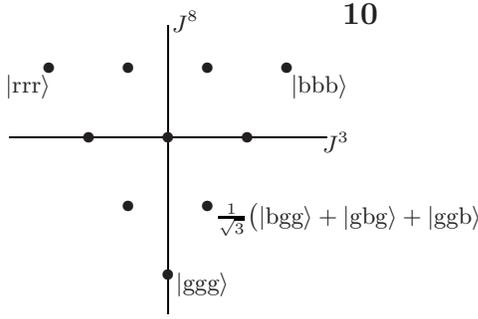
FIG. 8. Weight diagram of the representation **10**=(3,0). The weight diagram of the conjugate representation $\overline{\mathbf{10}}$=(0,3) is obtained by reflection at the origin (Ref. 67).

pling of the representations **6** and **3**, as can be seen from the Young tableaux in Fig. 4. On a more abstract level, the adjoint representation is the representation we obtain if we consider the generators J^a themselves basis vectors. In the weight diagram shown in Fig. 7, the generators J^3 and J^8 correspond to the two states at the origin, whereas the ladder operators $I^\pm$, $U^\pm$, and $V^\pm$ correspond to the states at the six surrounding points. In the notation of Fig. 7, the singlet orthogonal to **8** is given by $\frac{1}{\sqrt{3}}(|by\rangle+|rc\rangle+|gm\rangle)$.

The weight diagrams of four other representations relevant to our purposes below are shown in Figs. 8–10.

It is known that the physical properties of SU(2) spin chains crucially depend on whether the lattice sites are integer or half-integer spins. A similar distinction can be made for SU(3) chains, as elaborated in Sec. X. The distinction of integer or half-integer spin for SU(2) is replaced by a distinction between three families of irreducible representations of SU(3): either the number of boxes in the Young tableau is divisible by 3 without remainder (e.g., **1**, **8**, **10**, and **27**), with remainder 1 (e.g., **3**, $\overline{\mathbf{6}}$, **15**, and **15′**), or with remainder 2 (e.g., $\overline{\mathbf{3}}$, **6**, $\overline{\mathbf{15}}$, and $\overline{\mathbf{15}}′$).

While SU(2) has only one Casimir operator, SU(3) has two. The quadratic Casimir operator is defined as

$$J^2 = \sum_{a=1}^{8} J^a J^a, \tag{19}$$

where the J^a's are the generators of the representation. As J^2 commutes with all generators J^a, it is proportional to the identity for any finite-dimensional irreducible representation.
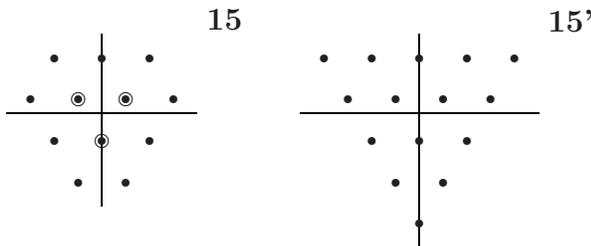
FIG. 9. Weight diagram of the representations **15**=(2,1) and **15′**=(4,0).
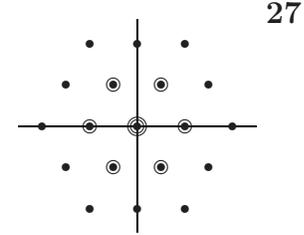
FIG. 10. Weight diagram of the self-conjugate representation **27**=(2,2). The state with $J^3=J^8=0$ is threefold degenerate (Ref. 67).

The eigenvalue in a representation with Dynkin coordinates (μ_1,μ_2) is[67]

$$J^2 = \mathcal{C}^2_{\mathrm{SU}(3)}(\mu_1,\mu_2) = \frac{1}{3}(\mu_1^2 + \mu_1\mu_2 + \mu_2^2 + 3\mu_1 + 3\mu_2). \tag{20}$$

We have chosen the normalization in Eq. (20) according to the convention

$$\mathcal{C}^2_{\mathrm{SU}(n)}(\text{adjoint representation}) = n,$$

which yields $\mathcal{C}^2_{\mathrm{SU}(3)}(1,1)$=3 for the representation **8**. Note that the quadratic Casimir operator cannot be used to distinguish between a representation and its conjugate. This distinction would require the cubic Casimir operator,[67] which we will not need for any of the models we propose below.

V. TRIMER MODEL (CONTINUED)

A. Verification of the model

We will now proceed with the verification of the trimer Hamiltonian [Eq. (12)]. Since the spins on the individual sites transform under the fundamental representation **3**, the SU(3) content of the four sites is

$$\mathbf{3} \otimes \mathbf{3} \otimes \mathbf{3} \otimes \mathbf{3} = 3 \cdot \mathbf{3} \oplus 2 \cdot \overline{\mathbf{6}} \oplus 3 \cdot \mathbf{15} \oplus \mathbf{15}', \tag{21}$$

i.e., we obtain representations **3** and $\overline{\mathbf{6}}$ and two nonequivalent 15-dimensional representations with Dynkin coordinates (2, 1) and (4, 0), respectively. All these representations can be distinguished by their eigenvalues of the quadratic Casimir operator, which is given by $(J_i^{(4)})^2$ if the four spins reside on the four neighboring lattice sites $i,\ldots,i+3$.

For the trimer states [Eq. (6)], the situation simplifies as we only have the two possibilities

$$\circ\!\!-\!\!\circ\!\!-\!\!\circ \quad \circ \quad \hat{=} \quad \mathbf{1} \otimes \mathbf{3} = \mathbf{3},$$
$$\circ\!\!-\!\!\circ \quad \circ\!\!-\!\!\circ \quad \hat{=} \quad \overline{\mathbf{3}} \otimes \overline{\mathbf{3}} = \mathbf{3} \oplus \overline{\mathbf{6}},$$

which implies that the total SU(3) spin on four neighboring sites can only transform under representations **3** or $\overline{\mathbf{6}}$. The eigenvalues of the quadratic Casimir operator for these representations are 4/3 and 10/3, respectively. The auxiliary operators

$$H_i = \left(\left(J_i^{(4)} \right)^2 - \frac{4}{3} \right) \left(\left(\mathbf{J}_i^{(4)} \right)^2 - \frac{10}{3} \right) \qquad (22)$$

hence annihilate the trimer states for all values of i, while they yield positive eigenvalues for **15** or **15**′, i.e., all other states. Summing H_i over all lattice sites i yields Eq. (12). We have numerically confirmed by exact diagonalization of Eq. (12) for chains with $N=9$ and 12 lattice sites that the three states [Eq. (7)] are the only ground states.

Note that the representation content of five neighboring sites in the trimer chains is just the conjugate of the above, as illustrated by

$$\circ\!\!-\!\!\circ\!\!\blacksquare\!\!\circ \quad \circ\!\!-\!\!\circ \qquad \hat{=} \quad \mathbf{1} \otimes \bar{\mathbf{3}} = \bar{\mathbf{3}},$$

$$\circ \quad \circ\!\!-\!\!\circ\!\!\blacksquare\!\!\circ \quad \circ \qquad \hat{=} \quad \mathbf{3} \otimes \mathbf{1} \otimes \mathbf{3} = \bar{\mathbf{3}} \oplus \mathbf{6}.$$

Since the quadratic Casimirs of conjugate representations have identical eigenvalues, $\mathcal{C}^2_{\text{SU}(3)}(\mu_1,\mu_2)=\mathcal{C}^2_{\text{SU}(3)}(\mu_2,\mu_1)$, we can construct another parent Hamiltonian for the trimer states Eq. (7) by simply replacing $\mathbf{J}_i^{(4)}$ with $\mathbf{J}_i^{(5)}$ in Eq. (12). This Hamiltonian will have a different spectrum. In comparison with the four-site interaction Hamiltonian [Eq. (12)], however, it is more complicated while bearing no advantages. We will not consider it further.

B. Elementary excitations

Let us now turn to the low-lying excitations of Eq. (12). In analogy with the MG model, it is evident that the SU(3) spinon or "coloron" excitations correspond to domain walls between the degenerate ground states. For the trimer model, however, there are two different kinds of domain walls, as illustrated by

$$\circ\!\!-\!\!\circ\!\!-\!\!\circ \quad \overset{\mathbf{3}}{\circ} \quad \circ\!\!-\!\!\circ\!\!-\!\!\circ \qquad (23)$$

$$\circ\!\!-\!\!\circ\!\!-\!\!\circ \quad \overset{\bar{\mathbf{3}}}{\circ\!\!-\!\!\circ} \quad \circ\!\!-\!\!\circ\!\!-\!\!\circ \qquad (24)$$

The first domain wall [Eq. (23)] connects ground state μ to the left to ground state $\mu+1$ to the right, where μ is defined modulo of 3 [see Eq. (7)], and consists of an individual SU(3) spin, which transforms under representation **3**. The second domain wall [Eq. (24)] connects ground state μ with ground state $\mu+2$. It consists of two antisymmetrically coupled spins on two neighboring sites and, hence, transforms under representation $\bar{\mathbf{3}}$. As we take momentum superpositions of the localized domain walls illustrated above, we expect one of them, but not both, to constitute an approximate eigenstate of the trimer model. The reason we do not expect both of them to yield a valid excitation is that they can decay into each other, i.e., if the representation **3** excitation is valid, the representation $\bar{\mathbf{3}}$ domain wall would decay into two representation **3** excitations and vice versa. The question which of the two excitations is the valid one, i.e., whether the elementary excitations transform under **3** or $\bar{\mathbf{3}}$ under SU(3) rotations, can be resolved through numerical studies. We will now discuss the results of these studies.

The representation **3** and the representation $\bar{\mathbf{3}}$ trial states
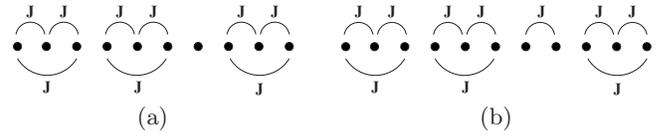
FIG. 11. Couplings used in the numerical studies to create (a) the localized representation **3** trial state and (b) the localized representation $\bar{\mathbf{3}}$ trial state.

require chains with $N=3\times\text{integer}+1$ and $N=3\times\text{integer}+2$ sites, respectively; we chose $N=13$ and $N=14$ for our numerical studies. To create the localized domain walls [Eqs. (23) and (24)], we numerically diagonalized auxiliary Hamiltonians with appropriate couplings, as illustrated in Fig. 11. From these localized excitations, we constructed momentum eigenstates by superposition and compared them to the exact eigenstates of our model Hamiltonian [Eq. (12)] for chains with the same number of sites. The results are shown in Table I and Fig. 12 for the representation **3** trial state and in Table II and Fig. 13 for the representation $\bar{\mathbf{3}}$ trial state.

The numerical results clearly indicate that the representation $\bar{\mathbf{3}}$ trial states [Eq. (24)] are valid approximations to the elementary excitations of the trimer chain, while the representation **3** trial states [Eq. (23)] are not. We deduce that the elementary excitations of the trimer chain [Eq. (12)] transform under $\bar{\mathbf{3}}$, that is, under the representation conjugated to the original SU(3) spins localized at the sites of the chain. Using the language of colors, one may say that if a basis for the original spins is spanned by blue, red, and green, a basis for the excitations is spanned by the complementary colors yellow, cyan, and magenta. This result appears to be a general feature of SU(3) spin chains, as it was recently shown explicitly to hold for the Haldane-Shastry model as well.[30–32]

Note that the elementary excitations of the trimer chain are deconfined, meaning that the energy of two localized representation $\bar{\mathbf{3}}$ domain walls or colorons [Eq. (24)] does not depend on the distance between them. The reason is simply that domain walls connect one ground state with another, without introducing costly correlations in the region between

TABLE I. Energies of the representation **3** trial states [Eq. (23)] in comparison to the exact excitation energies of the trimer model [Eq. (12)] and their overlaps for an SU(3) spin chain with $N=13$ sites.

| Momentum | E_{tot} | | % | |
($2\pi/N$)	Exact	Trial	off	Overlap
0	2.9735	4.5860	54.2	0.9221
1, 12	6.0345	10.2804	70.4	0.5845
2, 11	9.0164	17.2991	91.9	0.0
3, 10	6.6863	13.1536	96.7	0.0
4, 9	3.0896	5.0529	63.5	0.8864
5, 8	4.8744	7.5033	53.9	0.8625
6, 7	8.5618	16.6841	94.9	0.1095

FIG. 12. Dispersion of the representation **3** trial states [Eq. (23)] in comparison with the exact excitation energies of Eq. (12) for a chain with $N=13$. The lines are a guide for the eyes.

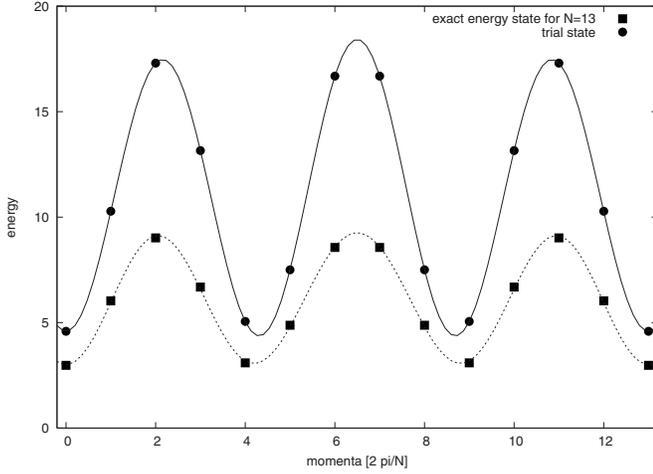FIG. 13. Dispersion of the representation $\overline{\mathbf{3}}$ trial states [Eq. (24)] in comparison with the exact excitation energies of Eq. (12) for a chain with $N=14$. The lines are a guide for the eyes.

the domain walls. In the case of the MG model and the trimer model introduced here, however, there is still an energy gap associated with the creation of each coloron, which is simply the energy cost associated with the domain wall.

In most of the remainder of this paper, we will introduce a family of exactly soluble valence bond models for SU(3) chains of various spin representations of the SU(3) spins at each lattice site. To formulate these models, we will first review Schwinger bosons for both SU(2) and SU(3) and the AKLT model.

VI. SCHWINGER BOSONS

Schwinger bosons[69,70] constitute a way to formulate spin-S representations of an SU(2) algebra. The spin operators

TABLE II. Energies of the representation $\overline{\mathbf{3}}$ trial states [Eq. (24)] in comparison with the exact excitation energies of the trimer model [Eq. (12)] and their overlaps for an SU(3) spin chain with $N=14$ sites.

| Momentum | E_{tot} | | % | |
$(2\pi/N)$	Exact	Trial	off	Overlap
0	2.1013	2.3077	9.8	0.9953
1, 13	4.3677	4.8683	11.5	0.9864
2, 12	7.7322	8.7072	12.6	0.9716
3, 11	6.8964	7.7858	12.9	0.9696
4, 10	3.2244	3.5415	9.8	0.9934
5, 9	2.2494	2.4690	9.7	0.9950
6, 8	5.4903	6.1016	11.1	0.9827
7	7.4965	8.5714	14.3	0.9562

$$S^x + iS^y = S^+ = a^{\dagger}b,$$

$$S^x - iS^y = S^- = b^{\dagger}a,$$

$$S^z = \tfrac{1}{2}(a^{\dagger}a - b^{\dagger}b) \tag{25}$$

are given in terms of boson creation and annihilation operators which obey the usual commutation relations

$$[a,a^{\dagger}] = [b,b^{\dagger}] = 1,$$

$$[a,b] = [a,b^{\dagger}] = [a^{\dagger},b] = [a^{\dagger},b^{\dagger}] = 0. \tag{26}$$

It is readily verified with Eq. (26) that S^x, S^y, and S^z satisfy Eq. (14). The spin quantum number S is given by half the number of bosons,

$$2S = a^{\dagger}a + b^{\dagger}b, \tag{27}$$

and the usual spin states (simultaneous eigenstates of S^2 and S^z) are given by

$$|S,m\rangle = \frac{(a^{\dagger})^{S+m}}{\sqrt{(S+m)!}} \frac{(b^{\dagger})^{S-m}}{\sqrt{(S-m)!}}|0\rangle. \tag{28}$$

In particular, the spin-$\tfrac{1}{2}$ states are given by

$$|\uparrow\rangle = c_{\uparrow}^{\dagger}|0\rangle = a^{\dagger}|0\rangle, \quad |\downarrow\rangle = c_{\downarrow}^{\dagger}|0\rangle = b^{\dagger}|0\rangle, \tag{29}$$

i.e., $a^{\dagger}$ and $b^{\dagger}$ act just like the fermion creation operators $c_{\uparrow}^{\dagger}$ and $c_{\downarrow}^{\dagger}$ in this case. The difference shows up only when two (or more) creation operators act on the same site or orbital. The fermion operators create an antisymmetric or singlet configuration (in accordance with the Pauli principle),

$$|0,0\rangle = c_{\uparrow}^{\dagger}c_{\downarrow}^{\dagger}|0\rangle, \tag{30}$$

while the Schwinger bosons create a totally symmetric or triplet (or higher spin if we create more than two bosons) configuration,

$$|1,1\rangle = \tfrac{1}{\sqrt{2}}(a^\dagger)^2|0\rangle,$$

$$|1,0\rangle = a^\dagger b^\dagger |0\rangle,$$

$$|1,-1\rangle = \tfrac{1}{\sqrt{2}}(b^\dagger)^2|0\rangle. \tag{31}$$

.

The generalization to SU(n) proceeds without incident. We content ourselves here by writing out explicitly the formalism for SU(3). In analogy to Eq. (25), we write the SU(3) spin operators [Eq. (9)],

$$J^1 + iJ^2 = I^+ = b^\dagger r,$$

$$J^1 - iJ^2 = I^- = r^\dagger b,$$

$$J^3 = \tfrac{1}{2}(b^\dagger b - r^\dagger r),$$

$$J^4 + iJ^5 = V^+ = b^\dagger g,$$

$$J^4 - iJ^5 = V^- = g^\dagger b,$$

$$J^6 + iJ^7 = U^+ = r^\dagger g,$$

$$J^6 - iJ^7 = U^- = g^\dagger r,$$

$$J^8 = \tfrac{1}{2\sqrt{3}}(b^\dagger b + r^\dagger r - 2g^\dagger g), \tag{32}$$

in terms of the boson annihilation and creation operators $b, b^\dagger$ (blue), $r, r^\dagger$ (red), and $g, g^\dagger$ (green) satisfying

$$[b,b^\dagger] = [r,r^\dagger] = [g,g^\dagger] = 1 \tag{33}$$

while all other commutators vanish. Again, it is readily verified with Eq. (33) that the operators J^a satisfy Eq. (17). The basis states spanning the fundamental representation **3** may, in analogy to Eq. (29), be written using either fermion or boson creation operators:

$$|b\rangle = c_b^\dagger |0\rangle = b^\dagger |0\rangle,$$

$$|r\rangle = c_r^\dagger |0\rangle = r^\dagger |0\rangle,$$

$$|g\rangle = c_g^\dagger |0\rangle = g^\dagger |0\rangle. \tag{34}$$

We write this abbreviated

$$\mathbf{3} = (1,0) = \square \,\hat{=}\, c_\alpha^\dagger |0\rangle = \alpha^\dagger |0\rangle. \tag{35}$$

The fermion operators can be used to combine spins transforming under the fundamental representation **3** antisymmetrically and, hence, to construct the representations

$$\mathbf{\bar 3} = (0,1) = \begin{array}{c}\square\\\square\end{array} \,\hat{=}\, c_\alpha^\dagger c_\beta^\dagger |0\rangle,$$

$$\mathbf{1} = (0,0) = \begin{array}{c}\square\\\square\\\square\end{array} \,\hat{=}\, c_b^\dagger c_r^\dagger c_g^\dagger |0\rangle. \tag{36}$$

The Schwinger bosons, by contrast, combine fundamental representations **3** symmetrically and, hence, yield represen-

tations labeled by Young tableaux in which the boxes are arranged in a horizontal row, like

$$\mathbf{6} = (2,0) = \square\square \;\hat{=}\; \alpha^\dagger \beta^\dagger |0\rangle,$$

$$\mathbf{10} = (3,0) = \square\square\square \;\hat{=}\; \alpha^\dagger \beta^\dagger \gamma^\dagger |0\rangle,$$

$$\mathbf{15'} = (4,0) = \square\square\square\square \;\hat{=}\; \alpha^\dagger \beta^\dagger \gamma^\dagger \delta^\dagger |0\rangle, \tag{37}$$

where $\alpha, \beta, \gamma, \ldots, \in \{b, r, g\}$. Unfortunately, it is not possible to construct representations such as

$$\mathbf{8} = (1,1) = \begin{array}{c}\square\square\\\square\end{array}$$

by simply taking products of anticommuting or commuting creation or annihilation operators.

VII. AKLT MODEL

Using the SU(2) Schwinger bosons introduced in the previous section, we may rewrite the Majumdar-Ghosh states [Eq. (1)] as

$$|\psi_{\mathrm{MG}}^{\substack{\mathrm{even}\\(\mathrm{odd})}}\rangle = \prod_{\substack{i\ \mathrm{even}\\(i\ \mathrm{odd})}} \left(a_i^\dagger b_{i+1}^\dagger - b_i^\dagger a_{i+1}^\dagger \right) |0\rangle$$

$$\equiv \Psi_{\mathrm{MG}}^{\substack{\mathrm{even}\\(\mathrm{odd})}} [a^\dagger, b^\dagger] \tag{38}$$

This formulation was used by Affleck *et al.*[15,16] to propose a family of states for higher spin representations of SU(2). In particular, they showed that the valance bond solid (VBS) state

$$|\psi_{\mathrm{AKLT}}\rangle = \prod_i \left(a_i^\dagger b_{i+1}^\dagger - b_i^\dagger a_{i+1}^\dagger \right) |0\rangle$$

$$= \Psi_{\mathrm{MG}}^{\mathrm{even}}[a^\dagger, b^\dagger] \cdot \Psi_{\mathrm{MG}}^{\mathrm{odd}}[a^\dagger, b^\dagger] |0\rangle$$

$$= \Big| \; \substack{\text{(diagram)}} \; \Big\rangle$$

projection onto spin $S=1$ \hfill (39)

is the exact zero-energy ground state of the spin-1 extended Heisenberg Hamiltonian

$$H_{\mathrm{AKLT}} = \sum_i \left(S_i S_{i+1} + \frac{1}{3}(S_i S_{i+1})^2 + \frac{2}{3} \right) \tag{40}$$

with periodic boundary conditions. Each term in the sum of Eq. (40) projects onto the subspace in which the total spin of a pair of neighboring sites is $S=2$. The Hamiltonian [Eq. (40)] thereby lifts all states except Eq. (39) to positive energies. The VBS state [Eq. (39)] is a generic paradigm as it shares all the symmetries, but, in particular, the Haldane spin gap,[8,9,34] of the spin-1 Heisenberg chain. It even offers a particularly simple understanding of this gap, or of the linear confinement potential between spinons responsible for it, as illustrated by the diagram

energy cost $\propto$ distance
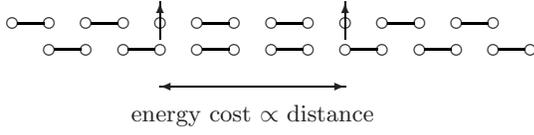
Our understanding[71,72] of the connection between the confinement force and the Haldane gap is that the confinement effectively imposes an oscillator potential for the relative motion of the spinons. We then interpret the zero-point energy of this oscillator as the Haldane gap in the excitation spectrum.

The AKLT state can also be written as a matrix product.[42,44,45] We first rewrite the valence bonds

$$(a_i^\dagger b_{i+1}^\dagger - b_i^\dagger a_{i+1}^\dagger) = (a_i^\dagger, b_i^\dagger)\begin{pmatrix} b_{i+1}^\dagger \\ -a_{i+1}^\dagger \end{pmatrix},$$

and then use the outer product to combine the two vectors at each site into a matrix

$$M_i \equiv \begin{pmatrix} b_i^\dagger \\ -a_i^\dagger \end{pmatrix}(a_i^\dagger, b_i^\dagger)|0\rangle_i = \begin{pmatrix} |1,0\rangle_i & \sqrt{2}|1,-1\rangle_i \\ -\sqrt{2}|1,1\rangle_i & -|1,0\rangle_i \end{pmatrix}. \tag{41}$$

Assuming PBCs, Eq. (39) may then be written as the trace of the matrix product

$$|\psi_{\text{AKLT}}\rangle = \text{tr}\left(\prod_i M_i\right). \tag{42}$$

.

In the following section, we will propose several exact models of VBSs for SU(3).

VIII. SU(3) VALENCE BOND SOLIDS

To begin with, we use SU(3) Schwinger bosons introduced in Sec. VI to rewrite the trimer states [Eq. (7)] as

$$|\psi_{\text{trimer}}^{(\mu)}\rangle = \prod_{\substack{i \\ [(i-\mu)/3 \text{ integer}]}} \left(\sum_{(\alpha,\beta,\gamma)=\pi(b,r,g)} \text{sgn}(\pi)\alpha_i^\dagger \beta_{i+1}^\dagger \gamma_{i+2}^\dagger\right)|0\rangle$$

$$\equiv \Psi^\mu[b^\dagger,r^\dagger,g^\dagger]|0\rangle, \tag{43}$$

where, as in Eq. (7), $\mu=1,2,3$ labels the three degenerate ground states, i runs over the lattice sites subject to the constraint that $\frac{i-\mu}{3}$ is integer, and the sum extends over all six permutations π of the three colors b, r, and g. This formulation can be used directly to construct VBSs for SU(3) spin chains with spins transforming under representations **6** and **10** on each site.

A. Representation 6 VBS

We obtain a representations **6** VBS from two trimer states by projecting the tensor product of two fundamental representations **3** onto the symmetric subspace, i.e., onto the **6** in the decomposition $\mathbf{3}\otimes\mathbf{3}=\bar{\mathbf{3}}\oplus\mathbf{6}$. Graphically, this is illustrated as follows:

one site

projection onto rep. $\mathbf{6} = (2,0)$ \hfill (44)
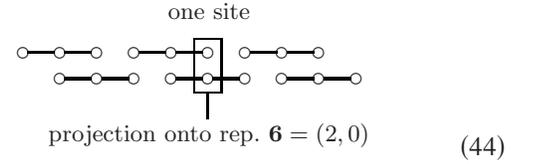
This construction yields three linearly independent **6** VBS states, as there are three ways to choose two different trimer states out of a total of three. These three VBS states are readily written out using Eq. (43),

$$|\psi_{6\text{VBS}}^{(\mu)}\rangle = \Psi^\mu[b^\dagger,r^\dagger,g^\dagger]\cdot\Psi^{\mu+1}[b^\dagger,r^\dagger,g^\dagger]|0\rangle \tag{45}$$

for $\mu=1$, 2, or 3. If we pick four neighboring sites on a chain with any of these states, the total SU(3) spin of those may contain the representations

 $\ \hat{=}\ \ \mathbf{3}\otimes\mathbf{3}\ =\ \bar{\mathbf{3}}\oplus\mathbf{6}$

or the representations

 $\ \hat{=}\ \ \bar{\mathbf{3}}\otimes\bar{\mathbf{3}}\otimes\mathbf{3}\ =\ 2\cdot\bar{\mathbf{3}}\oplus\mathbf{6}\oplus\overline{\mathbf{15}},$

i.e., the total spin transforms under $\bar{\mathbf{3}}$, **6**, or $\overline{\mathbf{15}}=(1,2)$, all of which are contained in the product

$$\mathbf{6}\otimes\mathbf{6}\otimes\mathbf{6}\otimes\mathbf{6}$$

$$= 3\cdot\bar{\mathbf{3}}\oplus 6\cdot\mathbf{6}\oplus 7\cdot\overline{\mathbf{15}}\oplus 3\cdot\overline{\mathbf{15}}'\oplus 3\cdot\mathbf{21}\oplus 8\cdot\mathbf{24}$$

$$\oplus 6\cdot\overline{\mathbf{42}}\oplus\mathbf{45}\oplus 6\cdot\mathbf{60}\oplus 3\cdot\mathbf{63} \tag{46}$$

and hence possible for a representation **6** spin chain in general. The corresponding Casimirs are given by $\mathcal{C}_{\text{SU(3)}}^2(0,1)=\frac{4}{3}$, $\mathcal{C}_{\text{SU(3)}}^2(2,0)=\frac{10}{3}$, and $\mathcal{C}_{\text{SU(3)}}^2(1,2)=\frac{16}{3}$. This leads us to propose the parent Hamiltonian

$$H_{6\text{VBS}} = \sum_{i=1}^N H_i, \tag{47}$$

with

$$H_i = \left(\left(J_i^{(4)}\right)^2 - \frac{4}{3}\right)\left(\left(J_i^{(4)}\right)^2 - \frac{10}{3}\right)\left(\left(J_i^{(4)}\right)^2 - \frac{16}{3}\right). \tag{48}$$

Note that the operators J_i^a, $a=1,\ldots,8$, are now given by 6×6 matrices, as the Gell-Mann matrices only provide the generators [Eq. (9)] of the fundamental representation **3**. Since the representations $\bar{\mathbf{3}}$, **6**, and $\overline{\mathbf{15}}$ possess the smallest Casimirs in the expansion [Eq. (46)], H_i and, hence, also $H_{6\text{VBS}}$ are positive semidefinite (i.e., have only non-negative eigenvalues). The three linearly independent states [Eq. (45)] are zero-energy eigenstates of [Eq. (47)].

To verify that these are the only ground states, we have numerically diagonalized Eq. (47) for $N=6$ and $N=9$ sites. For $N=9$, we find zero-energy ground states at momenta $k=0$, 3, and 6 (in units of $\frac{2\pi}{N}$ with the lattice constant set to unity). Since the dimension of the Hilbert space required the use of a Lanczos algorithm, we cannot be certain that there are no further ground states. We therefore diagonalized Eq.

(47) for $N=6$ as well, where we were able to obtain the full spectrum. We obtained five zero-energy ground states, two at momentum $k=0$ and one each at $k=2,3,4$. One of the ground states at $k=0$ and the $k=2,4$ ground states constitute the space of momentum eigenstates obtained by Fourier transform of the space spanned by the three **6** VBS states [Eq. (45)]. The remaining two states at $k=0,3$ are the momentum eigenstates formed by superposition of the state

$$i = 6 \quad 1 \quad 2 \quad 3 \quad 4 \quad 5 \quad 6 \quad 1 \tag{49}$$

and the same translated by one lattice spacing. It is readily seen that these two states are likewise zero-energy eigenstates of Eq. (47) for $N=6$ sites. The crucial difference, however, is that the **6** VBS states [Eq. (45)] remain zero-energy eigenstates of Eq. (47) for all N's divisible by 3, while the equivalent of Eq. (49) for larger N do not. We hence attribute these two additional ground states for $N=6$ to the finite size and conclude that the three states [Eq. (45)] are the only zero-energy ground states of Eq. (47) for general N's divisible by 3.

Excitations of the **6** VBS model are given by domain walls between two of the ground states [Eq. (45)]. As in the trimer model, two distinct types of domain walls exist, which transform according to representations $\bar{\mathbf{3}}$ and $\mathbf{3}$:

$$\tag{50}$$

It is not clear which excitation has the lower energy, and it appears likely that both of them are stable against decay. Let us first look at the representation. $\bar{\mathbf{3}}$ excitation. The four-site Hamiltonian [Eq. (48)] annihilates the state for all i's except the four sites in the dashed box in Eq. (50), which contains the representations

$$\bar{\mathbf{3}} \otimes \bar{\mathbf{3}} \otimes \bar{\mathbf{3}} \otimes \mathbf{3} \otimes \mathbf{3}$$

$$= 6 \cdot \bar{\mathbf{3}} \oplus 5 \cdot \mathbf{6} \oplus 6 \cdot \overline{\mathbf{15}} \oplus \overline{\mathbf{15}}' \oplus 2 \cdot \mathbf{24} \oplus \overline{\mathbf{42}},$$

i.e., the representations $\overline{\mathbf{15}}' = (0,4)$, $\mathbf{24} = (3,1)$ twice, and $\overline{\mathbf{42}} = (2,3)$ with Casimirs $\frac{28}{3}$, $\frac{25}{3}$, and $\frac{34}{3}$, respectively, in addition to representations annihilated by H_i. For the representation **3** excitation sketched on the right in Eq. (50), there are two sets of four neighboring sites not annihilated by H_i as indicated by the dashed and the dotted box. Each set contains the representations

$$\bar{\mathbf{3}} \otimes \mathbf{3} \otimes \mathbf{3} \otimes \mathbf{3} = 3 \cdot \bar{\mathbf{3}} \oplus 3 \cdot \mathbf{6} \oplus 2 \cdot \overline{\mathbf{15}} \oplus \mathbf{24},$$

i.e., only the representation **24** in addition to representations annihilated by H_i. For our parent Hamiltonian [Eq. (47)], it hence may well be that the representation **3** anticoloron has the lower energy, but it is all but clear that the representation

$\bar{\mathbf{3}}$ has sufficiently higher energy to decay. For general representation **6** spin chains, it may depend on the specifics of the model which excitation is lower in energy and whether the conjugate excitation decays or not.

Since the excitations of the representation **6** VBS chain are merely domain walls between different ground states, there is no confinement between them. We expect the generic antiferromagnetic representation **6** chain to be gapless, even though the model we proposed here has a gap associated with the energy cost of creating a domain wall.

B. Representation 10 VBS

Let us now turn to the **10** VBS chain, which is a direct generalization of the AKLT chain to SU(3). By combining the three different trimer states [Eq. (43)] for $\mu=1$, 2, and 3 symmetrically,

$$|\psi_{\mathbf{10}\mathrm{VBS}}\rangle = \Psi^1[b^\dagger, r^\dagger, g^\dagger] \cdot \Psi^2[b^\dagger, r^\dagger, g^\dagger] \cdot \Psi^3[b^\dagger, r^\dagger, g^\dagger]|0\rangle$$

$$= \prod_i \left(\sum_{(\alpha,\beta,\gamma)=\pi(b,r,g)} \mathrm{sgn}(\pi) \alpha_i^\dagger \beta_{i+1}^\dagger \gamma_{i+2}^\dagger \right)|0\rangle, \tag{51}$$

we automatically project out the representation **10** in the decomposition $\mathbf{3} \otimes \mathbf{3} \otimes \mathbf{3} = \mathbf{1} \oplus 2 \cdot \mathbf{8} \oplus \mathbf{10}$ generated on each lattice site by the three trimer chains. This construction yields a unique state, as illustrated by

$$\text{projection onto } \mathbf{10} = (3,0) \tag{52}$$

In order to construct a parent Hamiltonian, note first that the total spin on two (neighboring) sites of a representation **10** chain is given by

$$\mathbf{10} \otimes \mathbf{10} = \overline{\mathbf{10}} \oplus \mathbf{27} \oplus \mathbf{28} \oplus \mathbf{35}. \tag{53}$$

On the other hand, the total spin of two neighboring sites for the **10** VBS state can contain only the representations

$$\bar{\mathbf{3}} \otimes \bar{\mathbf{3}} \otimes \mathbf{3} \otimes \mathbf{3} = 2 \cdot \mathbf{1} \oplus 4 \cdot \mathbf{8} \oplus \mathbf{10} \oplus \overline{\mathbf{10}} \oplus \mathbf{27}, \tag{54}$$

as can be seen easily from the dashed box in the diagram above. (Note that this result is independent of how many sites we include in the dashed box.) After the projection onto representation **10** on each lattice site, we find that only representations $\overline{\mathbf{10}} = (0,3)$ and $\mathbf{27} = (2,2)$ occur for the total spin of two neighboring sites for the **10** VBS state. With the Casimirs $\mathcal{C}^2_{\mathrm{SU}(3)}(0,3)=6$ and $\mathcal{C}^2_{\mathrm{SU}(3)}(2,2)=8$, we obtain the parent Hamiltonian

$$H_{\mathbf{10}\text{VBS}} = \sum_{i=1}^{N} \left((\boldsymbol{J}_i \boldsymbol{J}_{i+1})^2 + 5\boldsymbol{J}_i \boldsymbol{J}_{i+1} + 6 \right), \qquad (55)$$

where the operators J_i^a, $a = 1, \ldots, 8$, are now 10×10 matrices, and we have used $\boldsymbol{J}_i^2 = 6$. $H_{\mathbf{10}\ \text{VBS}}$ is positive semidefinite and annihilates the **10** VBS state [Eq. (51)]. We assume that Eq. (51) is the only ground state of Eq. (55).

The Hamiltonian [Eq. (55)] provides the equivalent of the AKLT model,[15,16] whose unique ground state is constructed from dimer states by projection onto spin 1, for SU(3) spin chains. Note that as in the case of SU(2), it is sufficient to consider linear and quadratic powers of the total spin of only two neighboring sites. This is a general feature of the corresponding SU(n) models, as we will elaborate in the following section.

Since the **10** VBS state [Eq. (51)] is unique, we cannot have domain walls connecting different ground states. We hence expect the coloron and anticoloron excitations to be confined in pairs, as illustrated below. The state between the excitations is no longer annihilated by Eq. (55), as there are pairs of neighboring sites containing higher-dimensional representations, as indicated by the dotted box below. As the number of such pairs increases linearly with the distance between the excitations, the confinement potential depends linearly on this distance,

$$\text{energy cost} \propto \text{distance} \qquad (56)$$
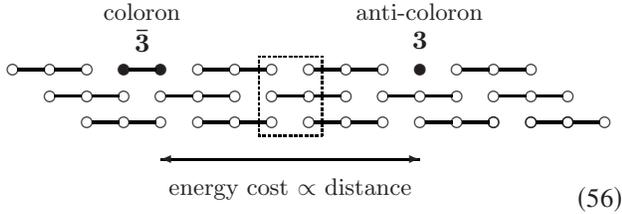
In principle, it would also be possible to create three colorons (or three anticolorons) rather than a coloron-anticoloron pair, but as all three excitations would feel strong confinement forces, we expect the coloron-anticoloron pair to constitute the dominant low-energy excitation. The confinement force between the pair induces a linear oscillator potential for the relative motion of the constituents. The zero-point energy of this oscillator gives rise to a Haldane-type energy gap (see Refs. 71 and 72 for a similar discussion in the two-leg Heisenberg ladder), which is independent of the model specifics. We expect this gap to be a generic feature of representation **10** spin chains with short-range antiferromagnetic interactions.

C. Representation 8 VBS

To construct a representation **8** VBS state, consider first a chain with alternating representations **3** and **$\bar{3}$** on neighboring sites, which we combine into singlets. This can be done in two ways, yielding the two states
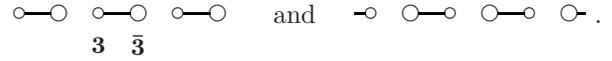
We then combine a **3**-**$\bar{3}$** state with an identical one shifted by one lattice spacing. This yields representations $\mathbf{3} \otimes \bar{\mathbf{3}} = \mathbf{1} \oplus \mathbf{8}$ at each site. The **8** VBS state is obtained by projecting onto representation **8**. Corresponding to the two **3**-**$\bar{3}$** states illustrated above, we obtain two linearly independent **8** VBS states, Ψ^L and Ψ^R, which may be visualized as

$$\text{projection onto } \mathbf{8} = (1, 1) \qquad (57)$$
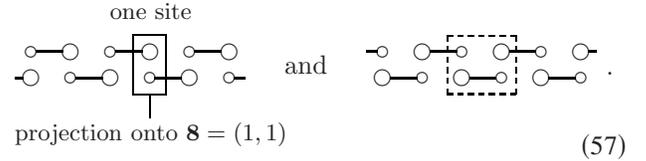
These states transform into each other under space reflection or color conjugation (interchange of **3** and **$\bar{3}$**).

It is convenient to formulate the corresponding state vectors as a matrix product. Taking (b,r,g) and (y,c,m) as bases for the representations **3** and **$\bar{3}$**, respectively, the singlet bonds in Ψ^L above can be written as

$$(|b\rangle_i |y\rangle_{i+1} + |r\rangle_i |c\rangle_{i+1} + |g\rangle_i |m\rangle_{i+1}) = (|b\rangle_i, |r\rangle_i, |g\rangle_i) \begin{pmatrix} |y\rangle_{i+1} \\ |c\rangle_{i+1} \\ |m\rangle_{i+1} \end{pmatrix}.$$

We are hence led to consider matrices composed of the outer product of these vectors on each lattice site,

$$M_i^{\mathbf{1} \oplus \mathbf{8}} = \begin{pmatrix} |y\rangle_i \\ |c\rangle_i \\ |m\rangle_i \end{pmatrix} (|b\rangle_i, |r\rangle_i, |g\rangle_i).$$

In the case of the AKLT model reviewed above, the Schwinger bosons take care of the projection automatically, and we can simply assemble these matrices into a product state. For the **8** VBS, however, we need to enforce the projection explicitly. This is most elegantly accomplished using the Gell-Mann matrices, yielding the projected matrix

$$M_i = \frac{1}{2} \sum_{a=1}^{8} \lambda^a \, \text{tr}(\lambda^a M_i^{\mathbf{1} \oplus \mathbf{8}}). \qquad (58)$$

Here, we have simply used the fact that the eight Gell-Mann matrices, supplemented by the unitary matrix, constitute a complete basis for the space of all complex 3×3 matrices. By omitting the unit matrix in the expansion [Eq. (58)], we effectively project out the singlet state. Written out explicitly, we obtain

$$M_i = \begin{pmatrix} \frac{2}{3}|by\rangle_i - \frac{1}{3}|rc\rangle_i - \frac{1}{3}|gm\rangle_i & |ry\rangle_i & |gy\rangle_i \\ |bc\rangle_i & -\frac{1}{3}|by\rangle_i + \frac{2}{3}|rc\rangle_i - \frac{1}{3}|gm\rangle_i & |gc\rangle_i \\ |bm\rangle_i & |rm\rangle_i & -\frac{1}{3}|by\rangle_i - \frac{1}{3}|rc\rangle_i + \frac{2}{3}|gm\rangle_i \end{pmatrix}. \tag{59}$$

Assuming PBCs, the **8** VBS state Ψ^L [illustrated in on the left of Eq. (57)] is hence given by the trace of the matrix product

$$|\psi^L_{\mathbf{8}\text{VBS}}\rangle = \text{tr}\left(\prod_i M_i\right). \tag{60}$$

To obtain the state Ψ^R [illustrated on the right of Eq. (57)], we simply have to transpose the matrices in the product,

$$|\psi^R_{\mathbf{8}\text{VBS}}\rangle = \text{tr}\left(\prod_i M_i^{\text{T}}\right). \tag{61}$$

Let us now formulate a parent Hamiltonian for these states. If we consider two lattice sites on an SU(3) chain with a representation **8** on each lattice site in general, we find the full SU(3) content

$$\mathbf{8} \otimes \mathbf{8} = \mathbf{1} \oplus 2 \cdot \mathbf{8} \oplus \mathbf{10} \oplus \overline{\mathbf{10}} \oplus \mathbf{27}, \tag{62}$$

with $\mathbf{10} = (3,0)$, $\overline{\mathbf{10}} = (0,3)$, and $\mathbf{27} = (2,2)$. On the other hand, for the **8** VBS states, only the representations $\mathbf{3} \otimes \overline{\mathbf{3}} = \mathbf{1} \oplus \mathbf{8}$ can occur for the total spin of two neighboring sites, as the two sites always contain one singlet [see dashed box in Eq. (57) on the right above]. With the Casimirs $\mathcal{C}^2_{\text{SU(3)}}(0,0)=0$ and $\mathcal{C}^2_{\text{SU(3)}}(1,1)=3$ for representations 1 and **8**, respectively, we construct the parent Hamiltonian

$$H_{\mathbf{8}\text{VBS}} = \sum_{i=1}^{N} \left((\boldsymbol{J}_i \boldsymbol{J}_{i+1})^2 + \frac{9}{2} \boldsymbol{J}_i \boldsymbol{J}_{i+1} + \frac{9}{2} \right), \tag{63}$$

where the operators J_i^a, $a=1,\ldots,8$, are now 8×8 matrices, and we have used the Casimir $\boldsymbol{J}_i^2 = 3$ on each site. $H_{\mathbf{8} \text{ VBS}}$ is positive semidefinite and annihilates the states Ψ^L and Ψ^R. We have numerically verified for chains with $N=3$, 4, 5, and 6 lattice sites that Ψ^L and Ψ^R are the only ground states of Eq. (63).

Naively, one might assume the **8** VBS model to support deconfined spinons or colorons, which correspond to domain walls between the two ground states Ψ^L and Ψ^R. A closer look at the domain walls, however, shows that this is highly unlikely, as each domain wall is a bound state of either two anticolorons or two colorons, as illustrated below,

(64)

There is no reason to assume that the domain wall depicted above as two anticolorons, in fact, corresponds to a single coloron, as it appears to be the case for the trimer chain.

There we created a domain wall corresponding to a single coloron by removing one of the representation **3** spins from a trimer, leaving the remaining representation **3** spins coupled antisymmetrically as in the ground state. If we were to combine the two representations **3** into a representation $\overline{\mathbf{3}}$ in Eq. (64), we would not reproduce a correlation present in the ground state but enforce a new correlation. The correct interpretation of the domain wall between Ψ^L and Ψ^R is hence that of a bound state between two linearly confined anticolorons. The origin of the confining potential is illustrated below,

(65)

As in the **10** VBS, the confinement induces a linear oscillator potential for the relative motion of the anti-colorons. The zero-point energy of this oscillator corresponds to a Haldane-type gap in the spectrum. The ground-state wave function of the oscillator is symmetric and, hence, corresponds to a symmetric combination of $\mathbf{3} \otimes \mathbf{3}$, i.e., representation **6**. The antisymmetric combination $\overline{\mathbf{3}}$ corresponds to the first excited state of the oscillator, which we expect to cost more than twice the energy of the symmetric state.[72] This statement holds for the pair of colorons in Eq. (64) as well.

The domain walls, however, are not the only low-energy excitations. In either of the ground states, we can create coloron-anticoloron bound states, which make no reference to the other ground state, as illustrated below,

(66)

The oscillator model tells us again that the "symmetric" combination of $\mathbf{3} \otimes \overline{\mathbf{3}}$, i.e., representation **8**, has the lowest energy, which we expect to be comparable, if not identical, to the energy required to create each of the domain walls above. The singlet **1** will have an energy comparable to that of a domain wall transforming under either $\overline{\mathbf{3}}$ or **3**. In any event, we expect the **8** VBS model to display a Haldane gap due to coloron confinement.

The excitation spectrum of Eq. (63) for a chain with $N=8$ sites and PBCs is shown in Fig. 14. The spectrum shows that the lowest excitation transforms under representation **8**, as expected from Eq. (66), with a singlet and then another representation **8** following at slightly higher energies. It is tempting to interpret those three levels as the lowest levels of the coloron-anticoloron oscillator [Eq. (66)], but then there should be another singlet at a comparable spacing above. The fact that the spacings between these excitations are significantly smaller than the energy of the first exited state, however, would be consistent with such an interpretation, as the spinons in VBS models always have a local energy cost associated with their creation, which is specific to these models and not related to the universal Haldane gap stemming from confinement forces.

Most importantly, the spectrum provides strong evidence in favor of our assumption that the domain walls are not elementary excitations, but bound states of either two colorons or two anticolorons, and hence that the lowest-energy excitations of finite chains are coloron-anticoloron bound states as illustrated in Eq. (66). The assumption is crucial for our conclusion that the model exhibits a Haldane gap. If the low-energy sector of the model was determined by two deconfined domain walls, we would see a continuum of states in the spectrum, similar to the spectrum seen in spin $S=\frac{1}{2}$ chains of SU(2). The well-defined low-energy modes in Fig. 14, however, look much more like the spinon-spinon bound state excitations seen in $S=1$ chains or two-leg $S=\frac{1}{2}$ Heisenberg ladders. In particular, if we assume that the individual domain walls transform under reps. **6** and $\bar{\mathbf{6}}$, we expect excitations transforming under the representations contained in $\mathbf{6} \otimes \bar{\mathbf{6}} = \mathbf{1} \oplus \mathbf{8} \oplus \mathbf{27}$ to be approximately degenerate. Fig. 14 shows clearly that such a multiplet is not present a the lowest energies.

IX. SU(n) MODELS

In this section, we generalize three of the models proposed for SU(3) spin chains, the trimer model, the symmetric representation **10** VBS, and the matrix product state **8** VBS to the case of SU(n) spin chains.

A. n-mer model

Consider an SU(n) spin chain with N sites, where N is a multiple of n, with a spin transforming according to the fundamental representation $\boldsymbol{n}$ of SU(n) at each lattice site,

$$\boldsymbol{n} = (1,0,\ldots,0) = \square \,\hat{=}\, c_\sigma^\dagger |0\rangle, \tag{67}$$

where σ denotes a "flavor," $\sigma \in \{f_1, \ldots, f_n\}$, and $c_\sigma^\dagger$ creates a fermion of flavor σ.

The SU(n) generators at site i are in analogy to Eq. (3) and (9) defined as

$$J_i^a = \frac{1}{2} \sum_{\sigma,\sigma'=f_1,\ldots,f_n} c_{i\sigma}^\dagger V_{\sigma\sigma'}^a c_{i\sigma'}, \quad a = 1, \ldots, n^2-1, \tag{68}$$

where the V^a denote the n^2-1 SU(n) Gell-Mann matrices.[73] The generators are normalized through the eigenvalue the quadratic Casimir operator takes in the adjoint representation, $\boldsymbol{J}^2 = \mathcal{C}_{\mathrm{SU}(n)}^2(1,0,\ldots,0,1) = n$.

To determine the eigenvalues of the quadratic Casimir for general representations of SU(n), a significant amount of representation theory is required.[74] We content ourselves here by providing the formulas up to $n=6$ in Appendix C.

In analogy to the trimer states [Eq. (7)], we construct the n-mer states of an SU(n) spin chain by combining sets of n neighboring spins into a singlet,

$$|\psi_{n\text{-mer}}^{(\mu)}\rangle = \prod_{\substack{i \\ [(i-\mu)/n \text{ integer}]}} \left(\sum_{(\sigma_1,\ldots,\sigma_n)=\pi(f_1,\ldots,f_n)} \mathrm{sgn}(\pi) \prod_{\kappa=1}^{n} c_{i-1+\kappa,\sigma_\kappa}^\dagger \right) |0\rangle, \tag{69}$$

where $\mu=1,\ldots,n$ labels the n degenerate ground states, and i runs over the lattice sites subject to the constraint that $\frac{i-\mu}{n}$ is integer. The sum extends over all $n!$ permutations π of the n flavors $f_1,\ldots,f_n$.

In order to identify a parent Hamiltonian, consider the total SU(n) spin on $n+1$ neighboring sites for the n-mer states. Following the rules of combining representations labeled by Young tableaux (see, e.g., Refs. 67 and 68), it is not difficult to see that the total spin will only contain representations given by tableaux with $n+1$ boxes and two columns, i.e., tableaux of the form

$\Big\}\ \nu$ rows
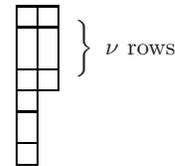
with $1 \leq \nu \leq \frac{n+1}{2}$. The eigenvalues of the quadratic Casimir operator for these representations are
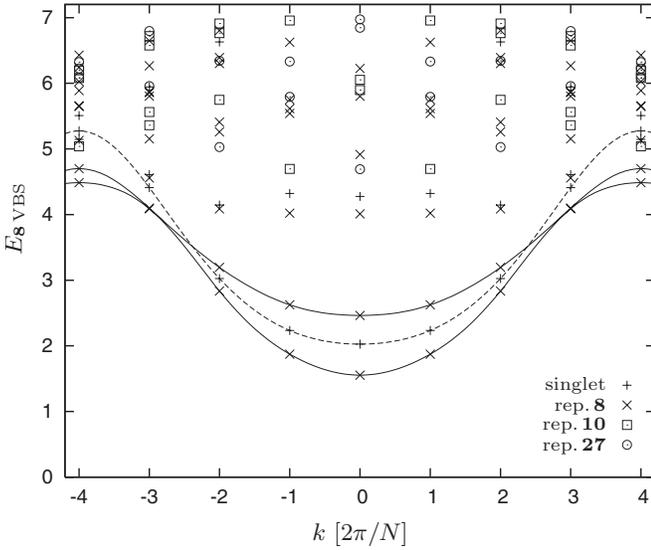
FIG. 14. Spectrum of the **8** VBS Hamiltonian [Eq. (63)] for N =8 sites obtained by exact diagonalization. (The lines are merely guides for the eyes.) The "magnon" excitation transforming under representation **8** of SU(3) has the lowest energy, followed by a singlet excitation, as expected from the discussion in the text. The well-defined modes at low energies provide strong evidence of coloron-anticoloron bound states as compared to deconfined domain walls and, hence, support our conclusion that the **8** VBS exhibits a Haldane gap due to spinon confinement.

$$f_n(\nu) = \frac{1}{2n}(n^2(2\nu - 1) - 2n(\nu - 1)^2 - 1). \qquad (70)$$

An educated guess for a parent Hamiltonian for the n-mer chain hence appears to be

$$H_{\text{trial}} = \sum_{i=1}^{N} H_i, \qquad (71)$$

with

$$H_i = \prod_{\nu=1}^{\lfloor(n+1)/2\rfloor} \left((\boldsymbol{J}_i^{(n+1)})^2 - f_n(\nu)\right), \qquad (72)$$

where $\lfloor\ \rfloor$ denotes the floor function, i.e., $\lfloor x \rfloor$ is the largest integer $l \leq x$, and we use the notation introduced in Eq. (11).

This construction yields the MG model[14] for SU(2), the trimer model [Eq. (12)] for SU(3), and a valid parent Hamiltonian for the four degenerate quadramer states for SU(4). For $n \geq 5$, however, the decomposition of the tensor product $\boldsymbol{n}^{\otimes(n+1)}$ contains irreducible representations corresponding to Young tableaux with more than two columns, whose Casimirs are equal or smaller than a number of Casimirs included in the list $f_n(\nu)$, $\nu = 1, 2, \ldots, \lfloor\frac{n+1}{2}\rfloor$. If the Casimir of such an "undesired" representation not included in the list is smaller than an odd number of Casimirs included in the list, we obtain negative eigenvalues for H_i, and it is not *a priori* clear anymore that the Hamiltonian [Eq. (71)] is positive semidefinite. An obvious cure to this problem is to write

$$H_{n\text{-mer}} = \sum_{i=1}^{N} H_i^2, \qquad (73)$$

with H_i as in Eq. (72). However, this does not cure potential problems arising from undesired representations which share the eigenvalues of the Casimir with one of the representations from the list, as it happens to be the case for $n=5$. The Hamiltonian [Eq. (73)] likewise annihilates these representations, giving rise to a remote possibility that the n-mer states [Eq. (69)] are not the only ground states of Eq. (73). The potential relevance of these problems has to be investigated for each n separately.

B. Representation $(n,0,\ldots,0)$ VBS

As a generalization of the AKLT model for SU(2) and the **10** VBS model for SU(3) discussed above, we now consider a VBS for an SU(n) chain of spins transforming under the symmetric representation

$$(n,0,\ldots,0) = \underbrace{\boxed{}}_{n\ \text{boxes}} \;\hat{=}\; b_{\sigma_1}^\dagger b_{\sigma_2}^\dagger \ldots b_{\sigma_n}^\dagger |0\rangle,$$

where each $b_\sigma^\dagger$, $\sigma \in \{f_1,\ldots,f_n\}$, is an SU($n$) Schwinger boson. The VBS state is obtained by combining n n-mer states [Eq. (69)] one for each $\mu = 1, \ldots, n$, in that the total spin on each lattice site is projected onto the symmetric representation $(n,0,\ldots,0)$. This yields

$$|\psi_{(n,0,\ldots,0)\text{VBS}}\rangle$$
$$= \prod_i \left(\sum_{(\sigma_1,\ldots,\sigma_n)=\pi(f_1,\ldots,f_n)} \text{sgn}(\pi) \prod_{\kappa=1}^n b_{i-1+\kappa,\sigma_\kappa}^\dagger\right)|0\rangle. \qquad (74)$$

Let us now construct a parent Hamiltonian for the symmetric VBS [Eq. (74)]. The total SU(n) spin of two neighboring sites of a representation $(n,0,\ldots,0)$ spin chain, in general, contains all the representations corresponding to Young tableaux with $2n$ boxes and at most two rows, i.e., all tableaux of the form

$$\underbrace{}_{n-\nu\ \text{columns}} \underbrace{}_{2\nu\ \text{boxes}}$$

The eigenvalues of the quadratic Casimir operator for these representations are given by

$$g_n(\nu) \equiv \mathcal{C}^2_{\text{SU}(n)}(2\nu, n-\nu, 0, \ldots, 0) = 2n^2 - 4n + \nu(\nu + 1). \qquad (75)$$

On the other hand, the total SU(n) spin of two neighboring sites of the representation $(n,0,\ldots,0)$ VBS [Eq. (74)] has to be contained in the product

$$\boxed{}^{\otimes n-1} \otimes \boxed{} \otimes \boxed{} \qquad (76)$$

As we project the spin on each lattice site onto the representation $(n, 0, \ldots, 0)$, only two these representations remain:

and

The eigenvalues of the quadratic Casimir operator are given by $g_n(0) = 2n(n-2)$ and $g_n(1) = 2(n-1)^2$, respectively. Hence, using $\boldsymbol{J}_i^2 = n(n-1)$, we obtain the parent Hamiltonian

$$H_{(n,0,\ldots,0)\text{VBS}} = \sum_{i=1}^{N} \left((\boldsymbol{J}_i \boldsymbol{J}_{i+1})^2 + (2n-1)\boldsymbol{J}_i \boldsymbol{J}_{i+1} + n(n-1) \right).$$

(77)

Since $g_n(0) \geq 0$ for $n \geq 2$ and $g_n(\nu)$ is a strictly increasing function of ν, the Hamiltonian [Eq. (77)] is positive semidefinite. For $n=2$, we recover the AKLT model [Eq. (40)] for $n=3$, we recover the **10** VBS model [Eq. (55)].

C. Example of a matrix product state

In principle, a matrix product VBS can be formulated on all SU(n) chains with spins transforming under the symmetric combination of any representation $\boldsymbol{m}$ and its conjugate representation $\bar{\boldsymbol{m}}$. Unless the representation $\boldsymbol{m}$ is self-conjugate, we obtain two inequivalent states, which transform into each other under space reflection. The construction of these is analogous to the **8** VBS introduced above, and likewise best illustrated as

one site

and

projection onto the symmetric
combination in $\boldsymbol{m} \otimes \bar{\boldsymbol{m}}$

(78)

The thick lines indicate that we combine pairs of neighboring representations $\boldsymbol{m}$ and $\bar{\boldsymbol{m}}$ into singlets. On each lattice site, we project onto the symmetric combination of $\boldsymbol{m}$ and $\bar{\boldsymbol{m}}$, as indicated. By "symmetric combination" we mean that if representations $\boldsymbol{m}$ and $\bar{\boldsymbol{m}}$ of SU(n) have Dynkin coordinates $(\mu_1, \mu_2, \ldots, \mu_{n-1})$ and $(\mu_{n-1}, \mu_{n-2}, \ldots, \mu_1)$, respectively, we combine them into the representation with Dynkin coordinates $(\mu_1 + \mu_{n-1}, \mu_2 - \mu_{n-2}, \ldots, \mu_{n-1} + \mu_1)$. In other words, we align the columns of both tableaux horizontally and, hence, obtain a tableau with twice the width, without ever adding a single box vertically to a column of the tableaux we started with. The states [Eq. (78)] we obtain are translationally invariant and we expect the parent Hamiltonians to involve nearest-neighbor interactions only.

In this section, we will formulate the simplest SU(n) model of this general family. We take $\boldsymbol{m}$ to be the representation formed by antisymmetrically combining $\kappa \leq \frac{n}{2}$ fundamental representations,

$$\boldsymbol{m} = [\kappa] \equiv (0, \ldots, 0, 1, 0, \ldots, 0) = \left. \begin{array}{c} \square \end{array} \right\} \kappa \text{ boxes ,}$$

κ-th entry

which implies that we consider a model with the representation corresponding to a Young tableaux with a column with $n - \kappa$ boxes to the left of a column with κ boxes at each lattice site:

$$[\kappa, n-\kappa] \equiv \left. \begin{array}{c} \square \end{array} \right\} \kappa \text{ rows}$$

The construction of the parent Hamiltonian is similar to the n-mer model above. The total spin on two neighboring lattice sites can only assume representations contained in $\boldsymbol{m} \otimes \bar{\boldsymbol{m}}$, i.e., representations corresponding to tableaux of the form

$$[\nu, n - \nu] = \left. \begin{array}{c} \square \end{array} \right\} \nu \text{ rows}$$

with $0 \leq \nu \leq \kappa$. The eigenvalues of the quadratic Casimir operator for these representations are

$$h_n(\nu) = \nu(n - \nu + 1).$$

(79)

The obvious proposal for a parent Hamiltonian is hence

$$H = \sum_{i=1}^{N} H_i, \quad H_i = \prod_{\nu=0}^{\kappa} \left((\boldsymbol{J}_i^{(2)})^2 - h_n(\nu) \right),$$

(80)

where $\lfloor x \rfloor$ denotes again the floor function. This Hamiltonian singles out the matrix product state [Eq. (78)] as unique ground states for $n \leq 5$ but suffers from the same shortcomings as Eq. (71) with Eq. (72) for $n \geq 6$.

X. SPINON CONFINEMENT AND THE HALDANE GAP

A. Affleck-Lieb theorem

For the generic SU(2) spin chain, Haldane[8,9] identified the O(3) nonlinear sigma model as the effective low-energy field theory of SU(2) spin chains and argued that chains with integer spin possess a gap in the excitation spectrum, while a topological term renders half-integer spin chains gapless.[10,11] The exact models for SU(2) spin chains we reviewed above, the MG and the AKLT chain, serve a paradigms to illustrate the general principle. Unfortunately, the effective field theory description of Haldane yielding the distinction between gapless half-integer spin chains with deconfined spinons and gapped integer spin chains with confined spinons cannot be directly generalized to SU(n) chains, as there is no direct equivalent of the CP^1 representation used in Haldane's analysis.

Nonetheless, there is a rigorous and rather general result for antiferromagnetic chains of SU(n) spins transforming under a representation corresponding to a Young tableau with a number of boxes not divisible by n: Affleck and Lieb[63] showed that if the ground state is nondegenerate and the Hamiltonian consists nearest-neighbor interactions only, then the gap in the excitation spectrum vanishes as $1/N$ (where N is the number of sites) in the thermodynamic limit. This result is fully consistent with the picture suggested by the models introduced above. Like the MG model, the trimer model and the representation **6** VBS have degenerate ground states and interactions which extend beyond the nearest neighbor, which implies that the theorem is not directly applicable.

On physical grounds, however, the statement that a given model is gapless (i.e., the excitation gap vanishes in the thermodynamic limit) implies that the spinons are deconfined. The reason is simply that if there was a confinement force between them, the zero-point energy associated with the quantum-mechanical oscillator of the relative motion between the spinons would inevitably yield an energy gap. The MG, the trimer, and the **6** VBS model constitute pedagogically valuable paradigms of deconfined spinons. Since the excitations in these models are literally domain walls between different ground states, no long-range forces can exist between them.

B. General criterion for spinon confinement

More importantly, however, the exact models we introduced above provide information about the models of SU(n) spin chains with representations corresponding to Young tableaux with a number of boxes divisible by n, i.e., models for which the Affleck-Lieb theorem is not applicable. We have studied two SU(3) models belonging to this family in Sec. VIII, the representation **10** VBS and the representation **8** VBS, and found that both have confined spinons or colorons and hence display a Haldane-type gap in the spectrum.

In this section, we will argue that models of antiferromagnetic chains of SU(n) spins transforming under a representation corresponding to a Young tableau consisting of a number of boxes λ divisible by n generally possess a Haldane-type gap due to spinon confinement forces.

We should caution immediately that our argument is based on several assumptions, which we consider reasonable, but which we are ultimately unable to prove.

The first, and also the most crucial, is the assumption that the question of whether a given model supports free spinon excitations can be resolved through study of the corresponding VBS state. This assumption definitely holds for SU(2) spin chains, where the MG model for $S = \frac{1}{2}$ indicates that the spinons are free, while the AKLT model for $S = 1$ serves as a paradigm for spinon confinement and hence the Haldane gap. The general conclusions we derived from our studies of the SU(3) VBSs above rely on this assumption. The numerical results we reported on the representation **8** VBS provide evidence that this assumption holds at least for this model.

Let us consider an SU(n) spin chain with spins transforming under a representation corresponding to Young tableau consisting of L columns with $\kappa_1 \leqslant \kappa_2 \leqslant \cdots \leqslant \kappa_L < n$ boxes each,

$$[\kappa_1, \kappa_2, \ldots, \kappa_L] \equiv \quad \text{(81)}$$

with a total number of boxes

$$\lambda = \sum_{l=1}^{L} \kappa_l$$

divisible by n. We denote the Dynkin coordinates of this representation by $(\mu_1, \mu_2, \ldots, \mu_{n-1})$, which implies

$$\sum_{i=1}^{n-1} \mu_i = L.$$

Note that this representation is, by definition, given by the maximally symmetric component of the tensor product of the individual columns,

$$[\kappa_1, \kappa_2, \ldots, \kappa_L] = \mathcal{S}([\kappa_1] \otimes [\kappa_2] \otimes \cdots \otimes [\kappa_L]). \quad \text{(82)}$$

For convenience, we denote the $\binom{n}{\kappa}$ dimensional representation $[\kappa]$ in this section as $\boldsymbol{\kappa}_l \equiv [\kappa_l] = \textcircled{l}$.

Since λ is divisible by n, it will always be possible to obtain a singlet from the complete sequence of representations $\boldsymbol{\kappa}_1, \boldsymbol{\kappa}_2, \ldots, \boldsymbol{\kappa}_L$ by combining them antisymmetrically. To be precise, when we write that we combine representations $\boldsymbol{\kappa}_1$ and $\boldsymbol{\kappa}_2$ antisymmetrically, we mean we obtain a new representation $[\kappa_1 + \kappa_2]$ by stacking the two columns with κ_1 and κ_2 boxes on top of each other if $\kappa_1 + \kappa_2 < n$ and a new representation $[\kappa_1 + \kappa_2 - n]$ if $\kappa_1 + \kappa_2 \geqslant n$. In equations, we write this as

$$\mathcal{A}([\kappa_1] \otimes [\kappa_2]) \equiv \begin{cases} [\kappa_1 + \kappa_2] & \text{for } \kappa_1 + \kappa_2 < n \\ [\kappa_1 + \kappa_2 - n] & \text{for } \kappa_1 + \kappa_2 \geqslant n. \end{cases}$$

(83)

Following the notation used above, we indicate the antisymmetric combination of representations $\boldsymbol{\kappa}_l$ by a line connecting them. In particular, we depict the singlet formed by combining $\boldsymbol{\kappa}_1, \boldsymbol{\kappa}_2, \ldots, \boldsymbol{\kappa}_L$ on different lattice sites as

$$\textcircled{1}\!\!-\!\!\textcircled{2}\!\!-\!\!\textcircled{3}\!-\cdots-\textcircled{L} \quad \text{(84)}$$

The understanding here is that we combine them in the order indicated by the line, i.e., in Eq. (84) we first combine $\boldsymbol{\kappa}_1$ and $\boldsymbol{\kappa}_2$, and then we combine the result with $\boldsymbol{\kappa}_3$, and so on. Depending on the order of the representations $\boldsymbol{\kappa}_l$ on the line, we obtain different, but not necessarily orthogonal, singlets. We assume that it is irrelevant whether we combine the representations starting from the left or from the right of the line, as the resulting state will not depend on it.

In general, it will be possible to construct a number $\leqslant \lambda/n$ of singlets out of various combinations of the $\boldsymbol{\kappa}$'s, one for each block of $\boldsymbol{\kappa}$'s for which the values of κ add up to n as we combine the representation in the order described above. In this case, we will be able to construct one VBS for each

singlet and subsequently combine them at each site symmetrically to obtain the desired representation [Eq. (81)]. The argument for spinon confinement we construct below will hold for each of the individual VBSs and, hence, for the combined VBS as well. It is, hence, sufficient for our purposes to consider situations where the entire sequence $\kappa_1, \kappa_2, \ldots, \kappa_L$ is needed to construct a singlet.

A possible VBS "ground state" for a representation corresponding to a Young tableau with $L=4$ columns is depicted below,

$$\text{projection onto representation} \quad [\kappa_1, \kappa_2, \kappa_3, \kappa_4] \tag{85}$$
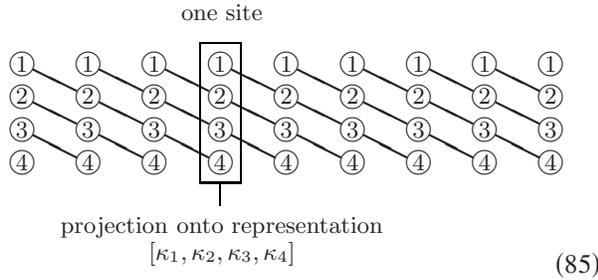
In general, there are as many inequivalent VBS "ground states" as there are inequivalent ways to order the representations $\kappa_1, \kappa_2, \ldots, \kappa_L$, i.e., the number of inequivalent VBS "ground states" is given by

$$\frac{L!}{\mu_1! \cdot \mu_2! \cdot \ldots \cdot \mu_{n-1}!}.$$

To give an example, the following VBS

$$\text{projection onto representation} \quad [\kappa_1, \kappa_2, \kappa_3, \kappa_4] \tag{86}$$
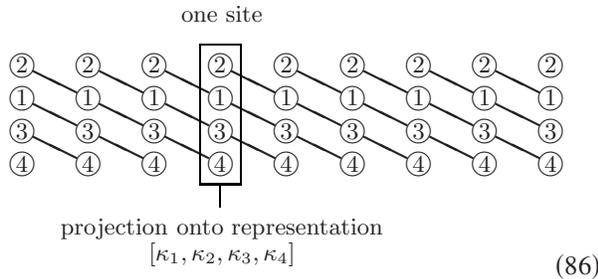
is inequivalent to the one above if and only if $\kappa_1 \neq \kappa_2$. Note that all these VBS "ground states" states are translationally invariant. We expect some of these states, but not all of them to be degenerate in energy for the appropriate parent Hamiltonian and have accordingly written ground states in quotation marks. For example, if we form an SU(4) VBS with representation $[\kappa_1, \kappa_2, \kappa_3] = [1, 1, 2]$, the combination
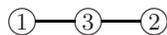
might yield a state with a lower energy for the appropriate Hamiltonian than the state formed by combining
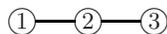
Simple examples where we have only two inequivalent VBS ground states are provided by the matrix product states discussed in Secs. VIII C and IX C.

We will now argue that the elementary excitations of the corresponding VBS models are always confined. To this end, we first observe that any domain wall between translationally invariant "ground states" consists of a total of $m \cdot n$ representations κ_l (m integer). To illustrate this, consider a domain wall between the "ground states" depicted in Eqs. (86) and (85):
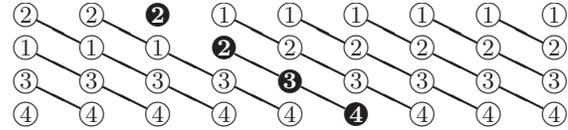
In the example, the domain wall consists of representations κ_2, κ_2, κ_3, and κ_4. If the translationally invariant states on both sites are true ground states, the domain wall is likely to correspond to two elementary excitations: a representation $\bar{\kappa}_1$ spinon consisting of an antisymmetric combination of a κ_2, a κ_3, and a κ_4, as indicated by the line in the drawing, and another representation κ_2 spinon. The reason we assume that κ_2, κ_3, and κ_4 form a representation $\bar{\kappa}_1$ is simply that this combination is present in both ground states on either side and, hence, bound to be the energetically most favorable combination. The second κ_2, however, is not part of this elementary excitation, as combining it antisymmetrically with the others (i.e., the $\bar{\kappa}_1$) would induce correlations which are not present in the ground state. We hence conclude that the second κ_2 is an elementary excitation as well. The domain wall depicted above consists of a spinon transforming under representation $\bar{\kappa}_1$ and an antispinon transforming under representation κ_2.

The next step in our argument is to note that the spinon and the complementary particle created simultaneously, which may either be its antiparticle or some other spinon, are confined through a linear potential. To see this, we pull them apart and look at the state in-between (color online):



$$\text{energy cost} \propto \text{distance} \tag{87}$$
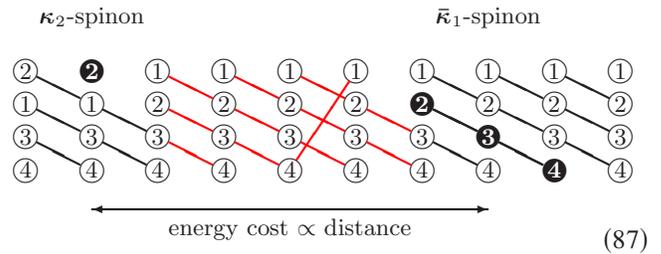
The state between spinon and antispinon is not translationally invariant. In the example, the unit cell of this state is depicted in red and consists of two regular bonds with three "singlet lines" between the sites, one stronger bond with four lines (which cross in the diagram) and one weaker bond with only two lines. If we assume that the two states [Eqs. (86) and (85)] on both sides are true ground states, it is clear that the irregularities in the strength of the bond correlations will cause the state between the spinon and antispinon to have a higher energy than either of them. This additional energy cost will induce a linear confinement potential between the spinons and, hence, a linear oscillator potential for the rela-

tive motion of the particles. As in the models studied above, the Haldane gap corresponds to the zero-point energy of this oscillator.

If one of the "ground states" to the left or to the right of the domain wall is not a true ground state but a translationally invariant state corresponding to a higher energy than the ground state, there will be a confining force between this domain wall and another domain wall which transforms the intermediate "ground state" with a higher energy back into a true ground state. This force will be sufficient to account for a Haldane gap, regardless of the strength or existence of a confinement force between the constituent particles of each domain wall.

The lowest-lying excitations of a representation $[\kappa_1, \kappa_2, \ldots, \kappa_L]$ spin chain, however, will, in general, not be domain walls but spinons created by breaking up one of the singlets [Eq. (84)] in a ground state. This is illustrated below for the ground state [Eq. (85)]:
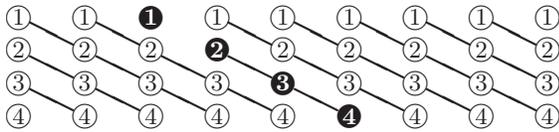
In the example, we have created a spinon transforming under representation $\bar{\kappa}_1$ and its antiparticle, a spinon transforming under representation κ_1. This is, however, irrelevant to the argument—we may break the singlet in any way we like. The important feature is that we obtain, by construction, at least two excitations and that these are confined. In our specific example, the confining potential is equivalent to the confining potential in Eq. (87) above (color online):
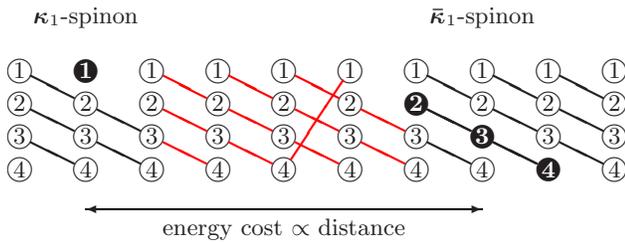
We leave it to the reader to convince himself or herself that the conclusions regarding confinement drawn from the simple examples studied here hold in general.

C. Models with confinement through interactions extending beyond nearest neighbors

Let us briefly summarize the results obtained. The SU(n) models we have studied so far fall into two categories. The models belonging to the first—the trimer chain, the **6** VBS, and the n-mer chain—have n degenerate ground states, which break translational invariance up to translations by n lattice spacings. The Young tableaux describing the representations of SU(n) at each site consist of a number of boxes λ which is smaller than n and, hence, obviously not divisible by n. The models support deconfined spinon excitations and, hence, do not possess a Haldane gap in the spectrum. The Hamiltonians of these models require interactions between

$n+1$ neighboring sites along the chain. Even though the Affleck-Lieb theorem is not directly applicable to the models we constructed above, it is applicable to SU(n) spin chains with spins transforming under the same representations. Like the VBS models, the theorem suggests that there is no Haldane gap in this family of models.

The models belonging to the second category—the **10** VBS, the **8** VBS, the representation $(n, 0, \ldots, 0)$ VBS, and the $\boldsymbol{m}$-$\bar{\boldsymbol{m}}$ matrix product state—have translationally invariant ground states. The ground states are unique for some models, such as the **10** and the $(n, 0, \ldots, 0)$ VBS, and degenerate for others, such as the **8** VBS. The Young tableaux describing the representations of SU(n) at each site consist of a number of boxes λ which is divisible by n. The Affleck-Lieb theorem is not applicable to models of this category. The spinon excitations for this category of models are subject to confinement forces, which give rise to a Haldane gap. The parent Hamiltonians for these models require interactions between nearest-neighbor sites only.

At first glance, this classification might appear complete. Further possibilities arise, however, in SU(n) spin chains where the number of boxes λ the Young tableau consists of and n have a common divisor different from n, which obviously requires that n is not a prime number. In this case, it is possible to construct VBS models in which the ground state breaks translational invariance only up to translations by n/q lattice spacings, where q denotes the largest common divisor of λ and n such that $q < n$. This implies that the ground state of the appropriate, translationally invariant Hamiltonian will be (n/q)-fold degenerate. In the examples we will elaborate on below, the parent Hamiltonians for these models require interactions between $\frac{n}{q}+1$ sites, a feature we conjecture to hold in general. The spinon excitations of these models are confined, even though the Affleck-Lieb theorem states that the nearest-neighbor Heisenberg chain of SU(n) spins transforming under these representations is gapless. (We implicitly assume here that the ground states of the SU(n) nearest-neighbor Heisenberg chains are nondegenerate.) Let us illustrate the general features of this third category of models with a few simple examples.

As a first example, consider an SU(4) chain with spins transforming under the ten-dimensional representation

$$(2, 0, 0) = \boxed{} \ .$$

Following the construction principle of the **6** VBS of SU(3), we find that the two degenerate VBS states illustrated through

one site

projection onto rep. $(2, 0, 0)$ (88)

are exact zero-energy ground states of

$$H_{(2,0,0)\text{VBS}} = \sum_{i=1}^{N} \left(\left(J_i^{(3)} \right)^4 - 12 \left(J_i^{(3)} \right)^2 + \frac{135}{4} \right), \quad (89)$$

which contains next-nearest-neighbor interactions.

The example illustrates the general rule stated above. The largest common divisor of $n=4$ and $\lambda=2$ is $q=2$. This implies $\frac{n}{q}=2$ and hence two degenerate VBS states which break translational invariance up to translations by two lattice spacings. The parent Hamiltonian requires interaction between three neighboring sites.

According to the Affleck-Lieb theorem, the models of antiferromagnetic SU(4) chains of representation (2,0,0) with nearest-neighbor Heisenberg interactions and nondegenerate ground states are gapless in the thermodynamic limit, which implies that the spinons are deconfined. In all the models we have studied in previous sections, the conclusions drawn from the Affleck-Lieb theorem were consistent with those drawn from our exact models. For the present model, however, they are not consistent.

Specifically, we strongly conjecture that the spinons in the (2,0,0) VBS are confined. This conjecture is based on the reasonable assumption that the elementary excitations of the model transform as either the fundamental representation **4** $=(1,0,0)$ of SU(4) or its conjugate representation $\bar{\mathbf{4}}$ $=(0,0,1)$. This assumption implies that a single domain wall in one of the 4-mer chains used to construct the VBS state [Eq. (88)] shifts this chain by one lattice spacing. If we assume a ground state to the left of the spinon, the state on to the right will have a higher energy for the next-nearest-neighbor Hamiltonian [Eq. (89)], as illustrated below,

$$\text{(90)}$$
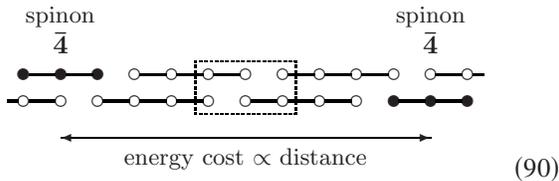
To recover the ground state, a second domain wall is required nearby, which is bound to the first by a linear potential.

Our conclusion is not in contradiction with the rigorous result of Affleck and Lieb, as they explicitly restrict themselves to models with nearest-neighbor interactions. If we had only nearest-neighbor interactions, the energy expectation value in the region between the domain walls would not be higher than in the ground state, as one can see easily from the diagram above—the sequence of alternating links would merely shift from (strong, weak, strong, weak) to (strong, strong, weak, weak).

As a second example, the situation is similar for an SU(6) chain with spins transforming under the 56-dimensional representation

$$(3,0,0,0,0) \;=\; \boxed{\;\;\;\;\;}\;.$$

With $n=6$ and $\lambda=3$, we have again $\frac{n}{q}=2$. Accordingly, we find that the two VBS states illustrated through

$$\text{(91)}$$
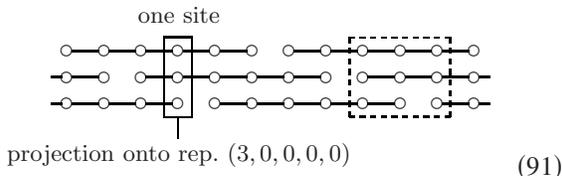
are exact ground states of a parent Hamiltonian containing up to next-nearest-neighbor interactions only and that the spinon excitations are confined.

As a third example, consider an SU(6) spin chain with spins transforming under the 21-dimensional representation

$$(2,0,0,0,0) \;=\; \boxed{\;\;}\;.$$

This implies $\frac{n}{q}=3$. We find that the three VBS states illustrated by


$$\text{(92)}$$
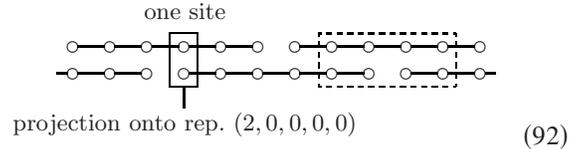
are exact ground states of a parent Hamiltonian involving the quadratic Casimir of total spin of four neighboring sites,

$$H_{(2,0,0,0,0)\text{VBS}} = \sum_{i=1}^{N} H_i, \tag{93}$$

with

$$H_i = \left(\left(J_i^{(4)}\right)^2 - \frac{32}{3}\right)\left(\left(J_i^{(4)}\right)^2 - \frac{44}{3}\right)\left(\left(J_i^{(4)}\right)^2 - \frac{50}{3}\right). \tag{94}$$

These VBS states break translational symmetry only up to translations by three lattice spacings. The spinons of this model are again confined through a linear potential, as illustrated below,

$$\text{(95)}$$
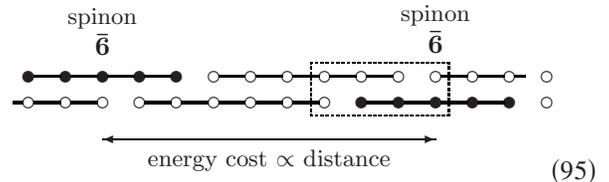
The conclusions we have drawn for this VBS model rest on the assumption that the quadratic Casimirs of the representations contained in the tensor product shown in the dashed box in Eq. (92) as well as in the tensor product one obtains if one shifts this box by one lattice spacing to the left or to the right are smaller than the largest Casimir contained in the tensor product shown in the dotted box in Eq. (95). We have verified the validity of this assumption for the (2,0,0,0,0) VBS model we considered here, but not shown it to hold for similar models with larger n or λ.
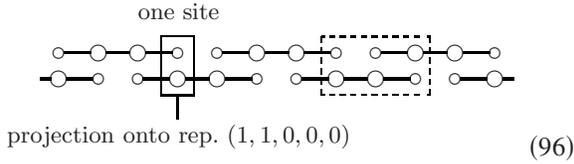
Finally, consider an SU(6) spin chain with spins transforming under the 70-dimensional representation

$$(1,1,0,0,0) \;=\; \boxed{\boxtimes}\;.$$

Thus, we have once again $\frac{n}{q}=2$. In a notation similar to the one introduced for the **8** VBS,

$$\square \ \hat{=} \ \circ, \quad \begin{array}{c}\square\\\square\end{array} \ \hat{=} \ \bigcirc,$$

the two degenerate VBSs are illustrated by

one site

projection onto rep. $(1,1,0,0,0)$ $\qquad$ (96)

are exact ground states of a parent Hamiltonian involving the quadratic Casimir of the total spin of three neighboring sites,

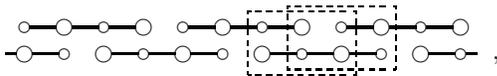$$H_{(1,1,0,0,0)\text{VBS}} = \sum_{i=1}^{N} H_i \qquad (97)$$

with

$$H_i = \left((\boldsymbol{J}_i^{(3)})^2 - 20\right)\left((\boldsymbol{J}_i^{(3)})^2 - 70\right)\left((\boldsymbol{J}_i^{(3)})^2 - 540\right). \quad (98)$$

The states [Eq. (96)] are not the only VBSs one can form. Other possibilities such as

or

however, contain additional representations for the total SU(6) spin of three neighboring sites and are, hence, expected to possess higher energies.

Spinon excitations transforming under the six-dimensional representation $(0,0,0,0,1)$ are linearly confined to spinons transforming under the 15-dimensional representation $(0,0,0,1,0)$:

spinon $\qquad\qquad$ spinon
$(0,0,0,0,1)$ $\qquad\qquad$ $(0,0,0,1,0)$

energy cost $\propto$ distance $\qquad$ (99)
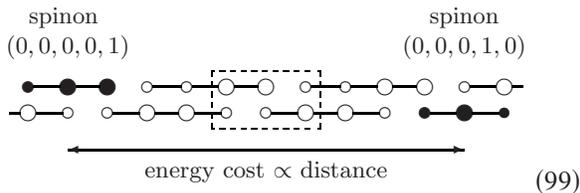
The VBS configuration we have drawn between the two spinons in Eq. (99) constitutes just one of several possibilities. We expect, however, that this possibility corresponds to the lowest energy among them for the Hamiltonian [Eq. (97)]. This concludes our list of examples.

The models introduced in this section are interesting in that they provide us with examples where spinon confinement, and with the confinement the existence of a Haldane gap, is caused by interactions extending beyond nearest neighbors. The conclusion drawn from the Affleck-Lieb theorem for SU(n) models with spins transforming under representations we have labeled here as the "third category" hence appear to hold for models with nearest-neighbor interactions only, to which the theorem is applicable. For these

models, the theorem states that the spectrum is gapless, which according to our understanding implies that the models support deconfined spinon excitations. The examples we have studied, by contrast, suggest that models with longer-ranged interactions belonging to this category exhibit confinement forces between the spinon excitations and hence possess a Haldane gap.

It is worth noting that even though in the examples we elaborated here $\lambda < n$, we expect our conclusions to hold for models with $\lambda > n$ as well. To see this, let $m > 0$ be an integer such that $nm < \lambda < n(m+1)$. We can now construct a first VBS with spinon confinement using nm boxes of the Young tableau and combine it with a second by projection on each side with a second VBS constructed from the remaining $\lambda' = \lambda - nm$ boxes. Since the spinons of the first VBS are always confined and hence gapped, the final VBS will support deconfined spinons if and only if the second VBS will support them, which, in turn, will depend on the largest common divisor q' of λ' and n as well as the range of the interaction. Since the largest common divisor q of n and λ is equal to q', there is no need to think in terms of λ' and q'. The conclusions regarding confinement and the Haldane gap will not depend on the distinction between λ and λ'.

D. Different categories of models

In this section, we used the rules emerging from the numerous examples we studied to argue that models of SU(n) spin chains, in general, fall into three categories. The classification depends on the number of boxes λ the Young tableau corresponding to the representation of the individual spins consists off, as follows:

(1) If λ and n have no common divisor, the models will support free spin excitations and, hence, not exhibit a Haldane gap. The general reasoning here is simply that the VBS states in this category break translational invariance up to translations by n lattice spacings and that there are (at least) n degenerate VBS ground states to each model. Spinons transforming under representations of Young tableaux with an arbitrary number of boxes can be accommodated in domain walls between these different ground states. Consequently, the spinons are deconfined.

(2) If λ is divisible by n, the general argument we have constructed in Sec. X B indicates that the model will exhibit spinon confinement and, hence, a Haldane gap.

(3) If λ and n have a common divisor different from n, the examples studied in Sec. X C suggest that the question of whether the spinons are confined or not depends on the details of the interactions. If q is the largest common divisor of λ and n, interactions ranging to the (n/q)th neighbor were required for spinon confinement in the models we studied. The Affleck-Lieb theorem,[63] on the other hand, tells us that SU(n) chains with nearest-neighbor Heisenberg interactions belonging to this category are gapless if the ground states are nondegenerate.

Note that the second category is really just the special case $q = n$ of the third: with $\frac{n}{q} = 1$, nearest-neighbor interac-

tions are already sufficient for spinon confinement and a Haldane gap.

The conclusion that interactions ranging to the (n/q)th neighbor are required for spinon confinement and a Haldane gap, however, is not universally valid. A counterexample is provided by the extended VBSs (XVBSs) introduced by Affleck, *et al.*[75] In this model, each site effectively takes the role of two neighboring sites when a VBS is constructed, and nearest-neighbor interactions are already sufficient to cause spinon confinement. We briefly review this model in the following section.

E. Counterexample: The SU(4) representation 6 extended VBS

In an article devoted to quantum antiferromagnets with spins transforming under the self-conjugate representations of SU($2n$), Affleck *et al.*[75] introduced an extended VBS for the six-dimensional SU(4) representation $(0, 1, 0)$. This representation is, with regard to the number of boxes the corresponding Young tableau consists of, not distinguishable from the symmetric representation **10** considered in Sec. X C, as both tableaux consist of two boxes:

$$\square \otimes \square = \square\square \oplus \begin{matrix}\square\\\square\end{matrix}$$
$$\mathbf{4} \quad \mathbf{4} \quad \mathbf{10} \quad \mathbf{6} \tag{100}$$

Since the two boxes are combined antisymmetrically for representation **6**, a VBS constructed along the lines of Sec. X C would no longer provide a paradigm for antiferromagnetic spin chains of the corresponding representation in general. Affleck *et al.*[75] have constructed an extended VBS, which is illustrated in the following diagram:

$$\tag{101}$$
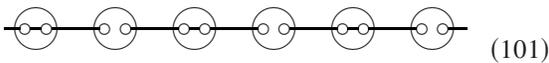
Here, each small circle represents a fundamental representation **4** of SU(4) (a box in the Young tableau), and each large circle a lattice site. The lines connecting four small circles indicate that these four fundamental representations are combined into an SU(4) singlet. The total spin of two neighboring sites in this state may assume the representations

$$\mathbf{4} \otimes \mathbf{\bar{4}} = \mathbf{1} \oplus \mathbf{15}, \tag{102}$$

while combining two representation **6** on neighboring sites, in general, yields

$$\mathbf{6} \otimes \mathbf{6} = \mathbf{1} \oplus \mathbf{15} \oplus \mathbf{20}. \tag{103}$$

To construct a parent Hamiltonian for the XVBS [Eq. (101)], it is hence sufficient to sum over projectors onto representation **20** on all pairs of neighboring sites. Using our conventions [Affleck *et al.*[75] have normalized the eigenvalues of the quadratic Casimir operator to $\mathcal{C}^2_{\mathrm{SU}(4)}$(adjoint representation) $=8$], the parent Hamiltonian takes the form

$$H_{\mathrm{XVBS}} = \sum_{i=1}^{N} \left(\boldsymbol{J}_i \boldsymbol{J}_{i+1} + \frac{1}{3}(\boldsymbol{J}_i \boldsymbol{J}_{i+1})^2 + \frac{5}{12} \right), \tag{104}$$

where the operators J_i^a, $a = 1, \ldots, 15$, are given by 6×6 matrices. Note that the ground state is twofold degenerate, as it breaks translational symmetry modulo translations by two lattice spacings.

We conjecture that the lowest-lying excitation is a bound state consisting of two fundamental representations **4**, which most likely are combined antisymmetrically into a representation **6**:

The SU(4) representation **6** XVBS provides us with an example where a nearest-neighbor Hamiltonian is sufficient to induce spinon confinement and a Haldane gap, even though the largest common divisor of $n=4$ and $\lambda=2$ is $q=2$, i.e., interactions including $\frac{n}{q}=2$ neighbors would be required following the rules derived from the examples in Sec. X C. The reason for this discrepancy is that in the XVBS model considered here, each site effectively takes the role of two neighboring sites. Affleck *et al.*[75,76] conjecture that the ground state of the SU(4) representation **6** nearest-neighbor Heisenberg model is, like the XVBS reviewed here, twofold degenerate, which implies that the Affleck-Lieb theorem is not applicable.

This example is valuable in showing that it is advisable to explicitly construct the VBS for a given representation of SU(n) in order to verify the applicability of the general rules motivated above.

XI. CONCLUSION

In the first part of this paper, we have formulated several exact models of SU(3) spin chains. We introduced a trimer model and presented evidence that the elementary excitations of the model transform under the SU(3) representations conjugate to the representation of the original spin on the chain. We then introduced three SU(3) valence bond solid chains with spins transforming under representations **6**, **10**, and **8**, respectively. We argued that of these four models, the coloron excitations are confined only in the **10** and the **8** VBS models, and that only those models with confined spinons exhibit a Haldane gap. We subsequently generalized three of our models to SU(n) and investigated again which models exhibit spinon confinement.

Finally, we used the rules emerging from the numerous examples we studied to argue that models of SU(n) spin chains, in general, fall into three categories with regard to spinon confinement and the Haldane gap. These are summarized in the previous section. The results rely crucially on the assumption that the conclusions we obtained for the VBS models we studied are of general validity. This assumption certainly holds for the corresponding SU(2) models and appears reasonable on physical grounds. Ultimately, however, it is only an assumption, or at best a hypotheses.

On a broader perspective, we believe that the models we have studied provide further indication that SU(n) spin

chains are an equally rich and rewarding subject of study as SU(2) spin chains have been since Bethe.

ACKNOWLEDGMENTS

APPENDIX A: PROPOSAL FOR AN EXPERIMENTAL REALIZATION OF SU(3) SPIN CHAINS IN AN OPTICAL LATTICE

In this appendix, we wish to describe a proposal for an experimental realization of SU(3) spin chains. The most eligible candidate for such experiments are ultracold gases in optical lattices. Recently, these systems have become an interesting playground for the realization of various problems of condensed-matter physics, such as the phase transition from a superfluid to a Mott insulator,[77,78] the fermionic Hubbard model,[79–81] and SU(2) spin chains.[82,83] In particular, the Hamiltonians for spin-lattice models may be engineered with polar molecules stored in optical lattices, where the spin is represented by a single-valence electron of a heteronuclear molecule.[84,85]

In a most naive approach, one might expect to realize an SU(3) spin (at a site in an optical lattice) by using atoms with three internal states, such as an atom with spin $S=1$. If now we were to interpret the $S^z=+1$ state as SU(3) spin "blue," the $S^z=0$ state as "red," and the $S^z=-1$ state as "green," however, the SU(3) spin would not be conserved. The SU(2) algebra would allow for the process $|+1,-1\rangle \rightarrow |0,0\rangle$, which in SU(3) language corresponds to the forbidden process $|b,g\rangle \rightarrow |r,r\rangle$.

A more sophisticated approach is hence required. One way to obtain a system with three internal states in which the number of particles in each state (i.e., of each color) is conserved is to manipulate an atomic system with total angular momentum $F=3/2$ (where $\mathbf{F}=\mathbf{S}_{el}+\mathbf{L}_{orb}+\mathbf{S}_{nuc}$ includes the internal spin of the electrons, the orbital angular momentum, and the spin of the nucleus) to simulate an SU(3) spin. The important feature here is that the atoms have four internal states, corresponding to $F^z=-\frac{3}{2},-\frac{1}{2},+\frac{1}{2},+\frac{3}{2}$. For such atoms, one has to suppress the occupation of one of the "middle" states, say, the $F^z=-\frac{1}{2}$ state, by effectively lifting it to a higher energy while keeping the other states approximately degenerate. This can be accomplished through a combination of an external magnetic field and two carefully tuned lasers, which effectively push down the energies of the $F^z=-\frac{3}{2}$ and the $F^z=+\frac{1}{2}$ states by coupling these states to states of (say) the energetically higher $F=5/2$ multiplet (see Fig. 15). At sufficiently low temperatures, we are hence left with a system with three internal states $F^z=-\frac{3}{2},+\frac{1}{2},+\frac{3}{2}$, which we may identify with the colors blue, red, and green of an SU(3) spin. In leading order, the number of particles of each color is now conserved, as required by SU(3) symmetry. For ex-
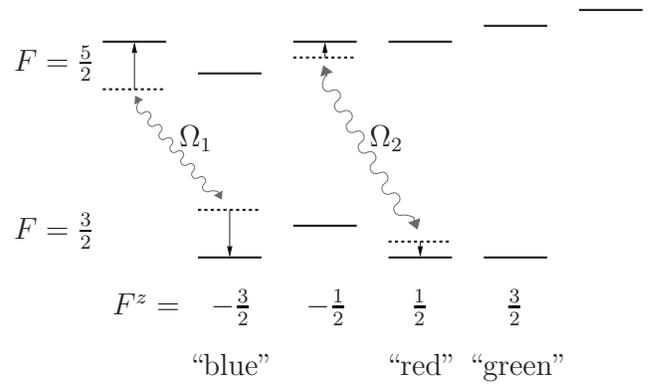

FIG. 15. Effective lifting of the $F^z=-\frac{1}{2}$ state.

ample, conservation of F^z forbids processes in which a blue and a green particle turn into two red ones, $|b,g\rangle \rightarrow |r,r\rangle$. Higher-order processes of the kind $|b,g,g\rangle \rightarrow |r,r,r\rangle$ are still possible but negligible if the experiment is conducted at sufficiently short time scales.

If one places fermionic atoms with an artificial SU(3) spin engineered along the lines of this or a related proposal in an optical lattice and allows for a weak hopping of the atoms on the lattice, one has developed an experimental realization of an SU(3) Hubbard model. If the energy cost U of having two atoms on the same lattice site is significantly larger than the hopping t and the density is one atom per site, the system will effectively constitute an SU(3) antiferromagnet. The dimension of this antiferromagnet will depend on the optical lattice, which can be one, two, or three dimensional.

In principle, the above proposal can be generalized to SU(n), even though the experimental obstacles are likely to grow "exponentially" with n. Besides, it is far from clear that such an endeavor is worthwhile, as all the nontrivial properties of SU(n) are already present in SU(3) chains [while SU(2) constitutes a special case].

APPENDIX B: GELL-MANN MATRICES

The Gell-Mann matrices are given by[67,68]

$$\lambda^1 = \begin{pmatrix} 0 & 1 & 0 \\ 1 & 0 & 0 \\ 0 & 0 & 0 \end{pmatrix}, \quad \lambda^2 = \begin{pmatrix} 0 & -i & 0 \\ i & 0 & 0 \\ 0 & 0 & 0 \end{pmatrix}, \quad \lambda^3 = \begin{pmatrix} 1 & 0 & 0 \\ 0 & -1 & 0 \\ 0 & 0 & 0 \end{pmatrix},$$

$$\lambda^4 = \begin{pmatrix} 0 & 0 & 1 \\ 0 & 0 & 0 \\ 1 & 0 & 0 \end{pmatrix}, \quad \lambda^5 = \begin{pmatrix} 0 & 0 & -i \\ 0 & 0 & 0 \\ i & 0 & 0 \end{pmatrix}, \quad \lambda^6 = \begin{pmatrix} 0 & 0 & 0 \\ 0 & 0 & 1 \\ 0 & 1 & 0 \end{pmatrix},$$

$$\lambda^7 = \begin{pmatrix} 0 & 0 & 0 \\ 0 & 0 & -i \\ 0 & i & 0 \end{pmatrix}, \quad \lambda^8 = \frac{1}{\sqrt{3}} \begin{pmatrix} 1 & 0 & 0 \\ 0 & 1 & 0 \\ 0 & 0 & -2 \end{pmatrix}.$$

They are normalized as $\text{tr}(\lambda^a \lambda^b)=2\delta_{ab}$ and satisfy the commutation relations $[\lambda^a,\lambda^b]=2f^{abc}\lambda^c$. The structure constants f^{abc} are totally antisymmetric and obey Jacobi's identity

$$f^{abc}f^{cde} + f^{bdc}f^{cae} + f^{dac}f^{cbe} = 0.$$

Explicitly, the nonvanishing structure constants are given by $f^{123} = i$, $f^{147} = f^{246} = f^{257} = f^{345} = -f^{156} = -f^{367} = i/2$, $f^{458} = f^{678} = i\sqrt{3}/2$, and 45 others obtained by permutations of the indices.

APPENDIX C: EIGENVALUES OF THE QUADRATIC CASIMIR OPERATOR

The eigenvalues of the quadratic Casimir operator for representations $\mathcal{C}^2_{SU(n)}(\mu_1, \mu_2, \ldots, \mu_{n-1})$ of SU(n) up to $n=6$ are given by

$$\mathcal{C}^2_{SU(2)}(\mu) = \tfrac{1}{4}(\mu^2 + 2\mu) = \frac{\mu}{2}\left(\frac{\mu}{2} + 1\right),$$

$$\mathcal{C}^2_{SU(3)}(\mu_1, \mu_2) = \tfrac{1}{3}(\mu_1^2 + \mu_1\mu_2 + \mu_2^2 + 3\mu_1 + 3\mu_2),$$

$$\mathcal{C}^2_{SU(4)}(\mu_1, \mu_2, \mu_3) = \tfrac{1}{8}(3\mu_1^2 + 4\mu_2^2 + 3\mu_3^2 + 4\mu_1\mu_2 + 2\mu_1\mu_3 + 4\mu_2\mu_3 + 12\mu_1 + 16\mu_2 + 12\mu_3),$$

$$\mathcal{C}^2_{SU(5)}(\mu_1, \mu_2, \mu_3, \mu_4) = \tfrac{1}{5}(2\mu_1^2 + 3\mu_2^2 + 3\mu_3^2 + 2\mu_4^2 + 3\mu_1\mu_2 + 4\mu_2\mu_3 + 3\mu_3\mu_4 + 2\mu_1\mu_3 + \mu_1\mu_4 + 2\mu_2\mu_4 + 10\mu_1 + 15\mu_2 + 15\mu_3 + 10\mu_4),$$

$$\begin{aligned}\mathcal{C}^2_{SU(6)}(\mu_1, \mu_2, \mu_3, \mu_4, \mu_5) = \tfrac{1}{12}(&5\mu_1^2 + 8\mu_2^2 + 9\mu_3^2 + 8\mu_4^2 + 5\mu_5^2 \\ &+ 8\mu_1\mu_2 + 12\mu_2\mu_3 + 12\mu_3\mu_4 \\ &+ 8\mu_4\mu_5 + 4\mu_1\mu_4 + 6\mu_1\mu_3 \\ &+ 8\mu_2\mu_4 + 6\mu_3\mu_5 + 4\mu_2\mu_5 \\ &+ 2\mu_1\mu_5 + 30\mu_1 + 48\mu_2 + 54\mu_3 \\ &+ 48\mu_4 + 30\mu_5).\end{aligned}$$

The general method to obtain these and further eigenvalues for $n > 6$ requires a discussion of representation theory[74] at a level which is beyond the scope of this paper.

The dimensionality of a representation $(\mu_1, \mu_2, \ldots, \mu_{n-1})$ is determined by the so-called Hook formula[67]

$$\dim = \frac{\displaystyle\prod_{i<j}^{n} (\lambda_i - \lambda_j + j - i)}{\displaystyle\prod_{i<j}^{n} (j - i)}, \tag{C1}$$

where $\lambda_i = \sum_{j=i}^{n-1} \mu_j$ for $i = 1, \ldots, n$. In particular, it yields for $n = 2, 3, 4$ the following:

$$\dim_{SU(2)}(\mu) = \mu + 1,$$

$$\dim_{SU(3)}(\mu_1, \mu_2) = \tfrac{1}{2}(\mu_1 + 1)(\mu_2 + 1)(\mu_1 + \mu_2 + 2),$$

$$\begin{aligned}\dim_{SU(4)}(\mu_1, \mu_2, \mu_3) = \tfrac{1}{12}&(\mu_1 + 1)(\mu_2 + 1)(\mu_3 + 1) \\ &\times (\mu_1 + \mu_2 + 2)(\mu_2 + \mu_3 + 2)(\mu_1 + \mu_2 \\ &+ \mu_3 + 3).\end{aligned}$$

[1] H. Bethe, Z. Phys. **71**, 205 (1931), translated in *The Many-Body Problem*, edited by D. C. Mattis (World Scientific, Singapore, 1993).

[2] C. N. Yang, Phys. Rev. Lett. **19**, 1312 (1967).

[3] R. J. Baxter, *Exactly Solved Models in Statistical Mechanics* (Academic, London, 1990).

[4] V. E. Korepin, N. M. Bogoliubov, and A. G. Izergin, *Quantum Inverse Scattering Method and Correlation Functions* (Cambridge University Press, Cambridge, 1997).

[5] L. D. Faddeev and L. A. Takhtajan, Phys. Lett. **85A**, 375 (1981).

[6] R. B. Laughlin, Phys. Rev. Lett. **50**, 1395 (1983).

[7] *Quantum Hall Effect*, edited by M. Stone (World Scientific, Singapore, 1992).

[8] F. D. M. Haldane, Phys. Lett. **93A**, 464 (1983).

[9] F. D. M. Haldane, Phys. Rev. Lett. **50**, 1153 (1983).

[10] I. Affleck, in *Fields, Strings and Critical Phenomena*, edited by E. Brézin and J. Zinn-Justin, Les Houches lectures Vol. XLIX (Elsevier, Amsterdam, 1990).

[11] E. Fradkin, *Field Theories of Condensed Matter Systems*, Frontiers in Physics No. 82 (Westview, Boulder, Co, 1991).

[12] A. O. Gogolin, A. A. Nersesyan, and A. M. Tsvelik, *Bosonization and Strongly Correlated Systems* (Cambridge University Press, Cambridge, 1998).

[13] T. Giamarchi, *Quantum Physics in One Dimension* (Oxford University Press, Oxford, 2004).

[14] C. K. Majumdar and D. K. Ghosh, J. Math. Phys. **10**, 1399 (1969).

[15] I. Affleck, T. Kennedy, E. H. Lieb, and H. Tasaki, Phys. Rev. Lett. **59**, 799 (1987).

[16] I. Affleck, T. Kennedy, E. H. Lieb, and H. Tasaki, Commun. Math. Phys. **115**, 477 (1988).

[17] F. D. M. Haldane, Phys. Rev. Lett. **60**, 635 (1988).

[18] B. S. Shastry, Phys. Rev. Lett. **60**, 639 (1988).

[19] F. D. M. Haldane, Phys. Rev. Lett. **66**, 1529 (1991).

[20] F. D. M. Haldane, Z. N. C. Ha, J. C. Talstra, D. Bernard, and V. Pasquier, Phys. Rev. Lett. **69**, 2021 (1992).

[21] F. D. M. Haldane, Phys. Rev. Lett. **67**, 937 (1991).

[22] Z. N. C. Ha and F. D. M. Haldane, Phys. Rev. B **47**, 12459 (1993).

[23] F. H. L. Eßler, Phys. Rev. B **51**, 13357 (1995).

[24] M. Greiter and D. Schuricht, Phys. Rev. B **71**, 224424 (2005).

[25] M. Greiter (unpublished).

[26] M. Greiter and D. Schuricht, Phys. Rev. Lett. (to be published).

[27] N. Kawakami, Phys. Rev. B **46**, 1005 (1992).

[28] N. Kawakami, Phys. Rev. B **46**, R3191 (1992).

[29] Z. N. C. Ha and F. D. M. Haldane, Phys. Rev. B **46**, 9359 (1992).

[30] P. Bouwknegt and K. Schoutens, Nucl. Phys. B **482**, 345 (1996).

[31] D. Schuricht and M. Greiter, Europhys. Lett. **71**, 987 (2005).

[32] D. Schuricht and M. Greiter, Phys. Rev. B **73**, 235105 (2006).

[33] R. Jullien and F. D. M. Haldane, Bull. Am. Phys. Soc. **28**, 344 (1983).

[34] I. Affleck, J. Phys.: Condens. Matter **1**, 3047 (1989).

[35] K. Okamoto and K. Nomura, Phys. Lett. A **169**, 433 (1992).

[36] S. Eggert, Phys. Rev. B **54**, R9612 (1996).

[37] S. R. White and I. Affleck, Phys. Rev. B **54**, 9862 (1996).

[38] D. Sen and N. Surendran, Phys. Rev. B **75**, 104411 (2007).

[39] S. Knabe, J. Stat. Phys. **52**, 627 (1988).

[40] M. Fannes, B. Nachtergaele, and R. F. Werner, Europhys. Lett. **10**, 633 (1989).

[41] W.-D. Freitag and E. Müller-Hartmann, Z. Phys. B: Condens. Matter **83**, 381 (1991).

[42] A. Klümper, A. Schadschneider, and J. Zittartz, J. Phys. A **24**, L955 (1991).

[43] T. Kennedy and H. Tasaki, Phys. Rev. B **45**, 304 (1992).

[44] A. Klümper, A. Schadschneider, and J. Zittartz, Z. Phys. B: Condens. Matter **87**, 281 (1992).

[45] A. Klümper, A. Schadschneider, and J. Zittartz, Europhys. Lett. **24**, 293 (1993).

[46] M. T. Batchelor and C. M. Yung, Int. J. Mod. Phys. B **8**, 3645 (1994).

[47] U. Schollwöck, T. Jolicoeur, and T. Garel, Phys. Rev. B **53**, 3304 (1996).

[48] A. Kolezhuk, R. Roth, and U. Schollwöck, Phys. Rev. Lett. **77**, 5142 (1996).

[49] A. K. Kolezhuk and U. Schollwöck, Phys. Rev. B **65**, 100401(R) (2002).

[50] B. Normand and F. Mila, Phys. Rev. B **65**, 104411 (2002).

[51] A. Läuchli, G. Schmid, and S. Trebst, Phys. Rev. B **74**, 144426 (2006).

[52] B. Sutherland, Phys. Rev. B **12**, 3795 (1975).

[53] T. C. Choy and F. D. M. Haldane, Phys. Lett. **90A**, 83 (1982).

[54] Y. Q. Li, M. Ma, D. N. Shi, and F. C. Zhang, Phys. Rev. B **60**, 12781 (1999).

[55] S. J. Gu and Y. Q. Li, Phys. Rev. B **66**, 092404 (2002).

[56] J. Damerau and A. Klümper, J. Stat. Mech.: Theory Exp. 2006, 1204.

[57] N. Kawashima and Y. Tanabe, Phys. Rev. Lett. **98**, 057202 (2007).

[58] A. Paramekanti and J. B. Marston, J. Phys.: Condens. Matter **19**, 125215 (2007).

[59] I. Affleck, Nucl. Phys. B **265**, 409 (1986).

[60] I. Affleck, Nucl. Phys. B **305**, 582 (1988).

[61] S. Chen, C. Wu, S. C. Zhang, and Y. Wang, Phys. Rev. B **72**, 214428 (2005).

[62] S. Chen, Y. Wang, W. Q. Ning, C. Wu, and H. Q. Lin, Phys. Rev. B **74**, 174424 (2006).

[63] I. Affleck and E. H. Lieb, Lett. Math. Phys. **12**, 57 (1986).

[64] M. Greiter, S. Rachel, and D. Schuricht, Phys. Rev. B **75**, 060401(R) (2007).

[65] P. M. van den Broek, Phys. Lett. **77A**, 261 (1980).

[66] T. Inui, Y. Tanabe, and Y. Onodera, *Group Theory and Its Applications in Physics* (Springer, Berlin, 1996).

[67] J. F. Cornwell, *Group Theory in Physics* (Academic, London, 1984), Vol. II.

[68] H. Georgi, *Lie Algebras in Particle Physics* (Addison-Wesley, Redwood City CA, 1982).

[69] J. Schwinger, in *Quantum Theory of Angular Momentum*, edited by L. Biedenharn and H. van Dam (Academic, New York, 1965).

[70] A. Auerbach, *Interacting Electrons and Quantum Magnetism* (Springer, New York, 1994).

[71] M. Greiter, Phys. Rev. B **65**, 134443 (2002).

[72] M. Greiter, Phys. Rev. B **66**, 054505 (2002).

[73] A. J. Macfarlane, A. Sudbery, and P. H. Weisz, Commun. Math. Phys. **11**, 77 (1968).

[74] J. E. Humphreys, *Introduction to Lie Algebras and Representation Theory* (Springer, New York, 1987).

[75] I. Affleck, D. P. Arovas, J. B. Marston, and D. A. Rabson, Nucl. Phys. **B366**, 467 (1991).

[76] J. B. Marston and I. Affleck, Phys. Rev. B **39**, 11538 (1989).

[77] D. Jaksch, C. Bruder, J. I. Cirac, C. W. Gardiner, and P. Zoller, Phys. Rev. Lett. **81**, 3108 (1998).

[78] M. Greiner, O. Mandel, T. Esslinger, T. W. Hänsch, and I. Bloch, Nature (London) **415**, 39 (2002).

[79] C. Honerkamp and W. Hofstetter, Phys. Rev. Lett. **92**, 170403 (2004).

[80] C. Honerkamp and W. Hofstetter, Phys. Rev. B **70**, 094521 (2004).

[81] A. Rapp, G. Zaránd, C. Honerkamp, and W. Hofstetter, Phys. Rev. Lett. **98**, 160405 (2007).

[82] L.-M. Duan, E. Demler, and M. D. Lukin, Phys. Rev. Lett. **91**, 090402 (2003).

[83] J. J. García-Ripoll, M. A. Martin-Delgado, and J. I. Cirac, Phys. Rev. Lett. **93**, 250405 (2004).

[84] A. Micheli, G. K. Brennen, and P. Zoller, Nat. Phys. **2**, 341 (2006).

[85] G. K. Brennen, A. Micheli, and P. Zoller, arXiv:quant-ph/0612180 (unpublished).